Met O (APR) Turbulence and Diffusion Note No. 210

Dispersion in Convective and Neutral Boundary Layers Using a Random Walk Model

by

B Hudson and D J Thomson

31 January 1994

Met O (APR)
(Atmospheric Processes Research)
Meteorological Office
London Road
Bracknell
Berks, RG12 2SZ

Note

This paper has not been published. Permission to quote from it should be obtained from the Assistant Director, Atmospheric Processes Research Division, Met O (APR), Meteorological Office, London Road, Bracknell, Berkshire, RG12 2SZ.

Met O (APR) Turbulence and Diffusion Note No. 210

Dispersion in Convective and Neutral Boundary Layers Using a Random Walk Model

by

B Hudson and D J Thomson

31 January 1994

Met O (APR)
(Atmospheric Processes Research)
Meteorological Office
London Road
Bracknell
Berks, RG12 2SZ

Note

Dispersion in convective and neutral boundary layers using a random walk model

by B.Hudson and D.J.Thomson

31st January 1994

Abstract

A series of random walk simulations of the dispersion of passive particles has been performed for a range of atmospheric stability conditions from free convection to neutral. The boundary layer was characterised using profiles of $\overline{w^2}$, $\overline{w^3}$ and ε, the rate of energy dissipation, from Mason's (1992) large eddy simulation (L.E.S.) studies. The particle trajectories were calculated numerically and were confined to the boundary layer by imposing reflections at the ground and at the boundary layer top. The resulting concentration fields and particle statistics were compared with the L.E.S. results and with the Willis and Deardorff (1976, 1978 and 1981) laboratory water tank experiments. Estimates of the optimum value of C_0, the coefficient relating the size of the random velocity increments to ε, were made for the different stability conditions by comparing the random walk simulations with the large-eddy simulations and with the tank experiments.

1 Introduction

Random walk models have proved to be valuable tools in the investigation of dispersion in the atmospheric boundary layer. Their flexibility means that dispersion can, in principle, be calculated in arbitrarily complex flows provided the mean flow, the turbulence statistics and the Lagrangian time scale are known.

The basis of the random walk approach consists of simulating numerically the trajectories of a large number of particles whose position and velocity are assumed to evolve in a Markovian manner. Each particle is envisaged as moving independently of the rest through a turbulent flow characterised by the relevant mean flow, turbulent statistics and Lagrangian time scale; one realisation of the flow is associated with each particle which is assumed to travel with the local fluid velocity, i.e. as a fluid element. The model ignores the correlation between the velocities of dispersing particles found in the real atmosphere and so cannot be used to calculate concentration fluctuations which depend on such correlations. The model can however be used to calculate ensemble mean concentrations

since these depend only on one-particle statistics. The ensemble mean concentration field is obtained by averaging over the ensemble of realisations and in stationary conditions is equivalent to a time-averaged concentration field. Because of the high Reynolds number in the atmospheric boundary layer, molecular diffusion can be ignored in the calculation of mean concentrations.

These ideas are expressed mathematically by a Langevin-type equation in which the particle's velocity increment is written as the sum of a deterministic term and a Gaussian random term. The condition that once a distribution of particles becomes well-mixed it must remain so is used in conjunction with the Fokker-Plank equation to constrain the form of the increments once $P(z,w)$, the vertical velocity probability density function for velocity w at height z, has been specified. Following Weil (1989), Luhar and Britter (1989) and others, $P(z,w)$ is written in terms of ${\sigma_w}^2 (\equiv \overline{w^2})$ and $\overline{w^3}$ as the sum of two Gaussian distributions. The random walk models produced by these authors simulate dispersion only in convective conditions; in this paper we extend this approach to derive a random walk model which can be used to simulate dispersion in a range of atmospheric stability conditions from free convection to neutral. This flexibility is achieved by relaxing the usual closure condition used in determining $P(z,w)$ that equates the modulus of the mean to the standard deviation in each of the two Gaussian distributions which make up $P(z,w)$; instead, in this paper use is made of a proportionality factor related to the vertical velocity skewness.

The model is tested against both L.E.S. model output and laboratory experimental results. The L.E.S. output comes from the recent work of Mason (1992) and provides both profiles of various turbulence statistics for input to the random walk model and concentration profiles to be compared with the random walk output for a range of atmospheric stabilities from free convective to neutral. Using the L.E.S. profiles in the random walk model allows direct comparisons to be made between the L.E.S. and random walk concentration fields. The model is also compared with the results of the laboratory dispersion studies of Willis and Deardorff (1976, 1978, 1981) which were performed to simulate dispersion in free convective conditions.

In order that the large scale features of the dispersion process were correctly simulated by the random walk model, the constant C_0, which relates the Lagrangian time scale to $\overline{w^2}$ and ε, was taken as a tunable parameter. The best value of C_0 for each of the stability categories and release heights was assessed by eye by comparing the plume characteristics with those obtained in the L.E.S. and in the water tank experiments.

2 Stochastic Model

The theory of random walk models is now well established and only a brief outline will be presented here; for more details see for example Legg and Raupach (1982), Van Dop et al (1985) and Thomson (1987). The approach adopted in this work follows that of Thomson (1987), Luhar and Britter (1989) and Weil(1989). Considering dispersion in the vertical direction only, the equations for the vertical velocity, w, and vertical displacement, z, of

a fluid element are given by

$$\left.\begin{aligned} dw &= a(z,w)dt + b(z,w)d\xi \\ dz &= wdt \end{aligned}\right\} \tag{1}$$

where $d\xi$ is the increment of a Wiener process – a Gaussian random forcing with zero mean and variance dt – and a and b are determined below.

To help in determining a and b it is useful to know the fixed point distribution of vertical velocities, $P(z,w)$. The updrafts and downdrafts that characterise the convective boundary layer result in the vertical velocity distribution at a fixed point being positively skewed (Lamb 1978; Willis and Deardorff 1978, 1981). A function $P(z,w)$ with this characteristic can be constructed as a sum of two Gaussian distributions,

$$P = AP_a + BP_b, \tag{2}$$

where

$$P_a = (\sqrt{2\pi}\sigma_a)^{-1} \exp\left(\frac{1}{2}\left[\frac{w-w_a}{\sigma_a}\right]^2\right)$$

and

$$P_b = (\sqrt{2\pi}\sigma_b)^{-1} \exp\left(\frac{1}{2}\left[\frac{w+w_b}{\sigma_b}\right]^2\right).$$

In order to specify P, the six parameters A, B, w_a, w_b, σ_a and σ_b need to be determined. Four constraints on the values of these parameters are provided by ensuring that the first four moments of the distribution are correct, i.e.

$$\int_{-\infty}^{\infty} w^n P(w,z)dw = \overline{w^n}(z)$$

where $\overline{w^0} = 1$, $\overline{w^1} = 0$ and $\overline{w^2}$ and $\overline{w^3}$ are to be specified. More explicitly we have

$$\left.\begin{aligned} \textstyle\int_{-\infty}^{\infty} P(w,z)dw = 1 \quad &\Rightarrow A + B = 1 \\ \textstyle\int_{-\infty}^{\infty} wP(w,z)dw = 0 \quad &\Rightarrow Aw_a - Bw_b = 0 \\ \textstyle\int_{-\infty}^{\infty} w^2P(w,z)dw = \overline{w^2} \quad &\Rightarrow A(\sigma_a^2 + w_a^2) + B(\sigma_b^2 + w_b^2) = \overline{w^2} \\ \textstyle\int_{-\infty}^{\infty} w^3P(w,z)dw = \overline{w^3} \quad &\Rightarrow A(3\sigma_a^2 w_a + w_a^3) - B(3\sigma_b^2 w_b + w_b^3) = \overline{w^3}. \end{aligned}\right\} \tag{3}$$

An extra constraint is needed for the solution of these equations and is usually taken to be $w_a = \sigma_a$ and $w_b = \sigma_b$ (Luhar and Britter, 1989 and Weil, 1989). In this work we use $w_a = \alpha\sigma_a$ and $w_b = \alpha\sigma_b$; α is allowed to vary to enable P to become close to Gaussian when the skewness is small (as in the neutral conditions). The equations (3) then become

$$\left.\begin{aligned} A + B &= 1 \\ A\sigma_a - B\sigma_b &= 0 \\ A\sigma_a^2 + B\sigma_b^2 &= \overline{w^2}/(1+\alpha) = \beta, \text{ say} \\ A\sigma_a^3 - B\sigma_b^3 &= \overline{w^3}/(3\alpha + \alpha^3) = \gamma, \text{ say} \end{aligned}\right\}$$

These equations can be solved to give

$$A = \sigma_b/(\sigma_a + \sigma_b), \quad B = \sigma_a/(\sigma_a + \sigma_b),$$

$$\sigma_a = \sigma_b + \gamma/\beta$$

and

$$\sigma_b = \frac{1}{2}\{\sqrt{\gamma^2/\beta^2 + 4\beta} - \gamma/\beta\}.$$

In neutral conditions P is observed to be close to Gaussian. In order to use the model to simulate dispersion in neutral conditions P must become Gaussian as $S \to 0$ where S is the skewness, $\overline{w^3}/\sigma_w^3$. This happens provided $\sigma_a \to \sigma_b$ and $w_a, w_b \to 0$ as $S \to 0$ and can be ensured in the model by adopting $\alpha = S^{1/3}$. In free convective conditions the resulting value of α is close to 1 ($\pm$ 20%) and so gives a P function very similar to that used in other work. Figure 1 shows the function P in neutral and convective stabilities.

The function $a(z,w)$ can be expressed in terms of b and P by the application of the 'well-mixed condition', i.e. the requirement that the model supports a steady distribution of particles in (z,w)-space with density proportional to $P(z,w)$. The distribution of particles in the model obeys the Fokker-Plank equation corresponding to the system (1) and so P is required to be a steady solution of this equation. Hence it is necessary that

$$\frac{\partial(wP)}{\partial z} + \frac{\partial(aP)}{\partial w} = \frac{1}{2}\frac{\partial^2}{\partial w^2}(b^2 P).$$

a is then given by

$$aP = \frac{\partial}{\partial w}\left(\frac{1}{2}b^2 P\right) + \phi \tag{4}$$

where ϕ satisfies

$$\frac{\partial(wP)}{\partial z} = -\frac{\partial \phi}{\partial w}. \tag{5}$$

Equation (5) and the requirement that $\phi \to 0$ as $|w| \to \infty$ are sufficient to determine ϕ.

To complete the model b needs to be specified. b can be written either in terms of the Lagrangian time scale τ - a measure of the time taken for particles to lose their memory of previous velocities - as $b = \sqrt{2\sigma_w^2/\tau}$ or in terms of ε as $b = \sqrt{C_0\varepsilon}$. The expression for b in terms of ε can be regarded either as an indirect way of estimating τ as $\tau = 2\sigma_w^2/C_0\varepsilon$ or as an attempt to ensure $\overline{(w(t+\delta t) - w(t))^2} \propto \varepsilon \delta t$ as predicted by inertial subrange theory, where $w(t)$ is the velocity following a particle. From the latter viewpoint C_0 should be a universal constant while in the former view there is no special reason to expect this. The former view point is perhaps more appropriate for the prediction of mean concentrations while the latter would give a more accurate description of the short time scale structure of particle trajectories. With the former view there is evidence to suggest C_0 varies according to the stability conditions being modelled. C_0 is usually taken equal to 2.0 in the simulation of convective boundary layers (Weil, 1989 and Luhar and Britter, 1989) while higher values are found to be necessary for neutral conditions. For example Sawford and Guest (1988) find values of 5 to 10 are necessary to give agreement with experimental measurements of dispersion. Also the theory of Rodean (1991) for C_0 in neutral conditions gives $C_0 = 2(\sigma_w/u_*)^4$ which, assuming $\sigma_w = 1.3u_*$, gives $C_0 = 5.7$.

Using Rodean's approach it is possible to obtain a theoretical prediction of how C_0 may vary with stability. C_0 can be written as $C_0 = 2\sigma_w^2/\varepsilon\tau$ and, by expressing τ in terms of an eddy diffusivity K_H via $K_H = \sigma_w^2\tau$ and adopting standard surface layer forms for σ_w, ε and K_H, it is possible to estimate C_0. Using the surface layer forms adopted in the UK Atmospheric Dispersion Modelling System (Carruthers et al 1992),

i.e. $\sigma_w^2 = u_*^2[1.69 + 3.25(z/|L|)^{2/3}]$, $\epsilon = u_*^3(1/kz + 1/|L|)$ and $K_H = ku_*z(1 + 16z/|L|)^{1/2}$, C_0 is found to vary as

$$\frac{2(1.69 + 3.25(z/|L|)^{2/3})^2}{(1 + kz/|L|)(1 + 16z/|L|)^{1/2}}. \tag{6}$$

In the neutral case the terms involving $|L|$ tend to zero giving Rodean's value. As $|L|$ becomes small and the flow becomes more convective the expression will tend to zero, although this limit is almost certainly incorrect (being caused by the failure of our expression for K_H to follow free convective scaling). For realistic values of $z/|L|$ (in the range 0 to 400) equation (6) increases from 5.7 at $z/|L| = 0$ to a maximum of 9.3 at $z/|L| = 3.9$ before decreasing to 4.9 at $z/|L| = 400$. The expression does not predict a gradual decrease in C_0 to the value 2.0 generally used in free convective simulations. In this work C_0 is taken as an adjustable parameter and the values found necessary for good dispersion results will be compared with equation (6).

Using $b = \sqrt{2\sigma_w^2/\tau}$ in equation (4) gives

$$a = \frac{1}{P}\left(-\frac{\sigma_w^2}{\tau}Q + \phi\right)$$

where Q is defined as

$$Q = AP_a\frac{(w - w_a)}{\sigma_a^2} + BP_b\frac{(w + w_b)}{\sigma_b^2}$$

and ϕ is defined as

$$\phi = -\frac{1}{2}\left(1 + \mathrm{erf}\frac{v_a}{\sqrt{2}}\right)\frac{\partial}{\partial z}(Aw_a) + \frac{1}{2}\left(1 + \mathrm{erf}\frac{v_b}{\sqrt{2}}\right)\frac{\partial}{\partial z}(Bw_b)$$

$$+P_a\sigma_a\left\{\left(\frac{\partial}{\partial z}(A\sigma_a) + \frac{w_aA}{\sigma_a}\frac{\partial w_a}{\partial z}\right) + \left(A\frac{\partial w_a}{\partial z} + \frac{w_aA}{\sigma_a}\frac{\partial \sigma_a}{\partial z}\right)v_a + A\frac{\partial \sigma_a}{\partial z}v_a^2\right\}$$

$$+P_b\sigma_b\left\{\left(\frac{\partial}{\partial z}(B\sigma_b) + \frac{w_bB}{\sigma_b}\frac{\partial w_b}{\partial z}\right) - \left(B\frac{\partial w_b}{\partial z} + \frac{w_bB}{\sigma_b}\frac{\partial \sigma_b}{\partial z}\right)v_b + B\frac{\partial \sigma_b}{\partial z}v_b^2\right\}$$

with

$$v_a = \frac{(w - w_a)}{\sigma_a}, \text{ and } v_b = \frac{(w + w_b)}{\sigma_b}.$$

This reduces to the free convective expression given by Luhar and Britter (1989) and Weil (1989) when $w_a = \sigma_a$ and $w_b = \sigma_b$.

3 Application of the Model

The application of equations (1) requires the specification of the profiles of the turbulence quantities $\overline{w^2}$, $\overline{w^3}$ and τ in the boundary layer. In the work presented here use is made of profiles obtained from Mason's (1992) recent simulations of dispersion using the L.E.S. technique. These simulations were performed to simulate the dispersion of particles in a range of atmospheric stabilities from free convective to neutral – seven runs were performed in total with each one corresponding to a different stability condition.

The L.E.S. $\overline{w^2}$ statistic has both a resolved and a subgrid component; the value of $\overline{w^2}$ used in the random walk model was generally taken to be the sum of these although a few runs were carried out with $\overline{w^2}$ taken to be just the resolved component. At the ground the turbulent eddies are small and so the resolved component, but not the sub-grid component, is zero. The L.E.S. $\overline{w^3}$ statistic also involves resolved and subgrid components and is given as $\overline{w^3} = \overline{w_R^3} + 3\overline{w_R w_{SG}^2} + 3\overline{w_R^2 w_{SG}} + \overline{w_{SG}^3}$ where w_R and w_{SG} denote the resolved and subgrid vertical velocities. The third term in this expression is equal to zero while the fourth term is difficult to estimate and is set equal to zero leaving the L.E.S. $\overline{w^3}$ as the sum of the first two terms, i.e. the third moment of the resolved motions and the correlation between the resolved w and the local subgrid velocity variance. At the ground both of these terms are zero. In the L.E.S. model the eddy viscosity and diffusivity remove kinetic energy from the resolved motions and potential energy from the resolved buoyancy field. In reality this energy would appear as small scale subgrid motions and would eventually be dissipated. Here, consistent with the assumptions in the subgrid model, we assume local equilibrium and estimate the energy dissipation rate directly as the sum of the energy lost through eddy viscosity and diffusivity. The Lagrangian time scale τ is calculated using ε through the relation $\tau = 2\sigma_w^2 / C_0 \varepsilon$. τ is set equal to zero at the ground and increases to a maximum in the middle of the boundary layer before falling to a minimum close to the boundary layer top. Except in the neutral case where the domain lid and the boundary layer top coincide, above this minimum τ increases very rapidly with height. In comparisons with experimental data the L.E.S. turbulence profiles for convective conditions have proved successful in that they are able to give a good measure of these statistics over a range of stabilities; the profiles for the neutral case are not as successful, probably because of insufficient resolution.

The boundary layer in the random walk model is defined between the heights $z = 0$, the ground, and $z = z_i$, the boundary layer top. In order to prevent τ (and thus Δt, the time step in the random walk model) from becoming too small and also to prevent particles escaping out of the model domain, particles within 1m of either of these limits are perfectly reflected to put them back into the model boundary layer. The value of z_i for the six convective simulations was taken as the height of the L.E.S. heat flux minimum. The L.E.S. concentration profiles show that only a few particles reach higher than this and only at very large times; also at this height the turbulence has fallen to low levels. Defined in this way, z_i is within 10% of Mason's Z_c, which is defined as twice the mean particle height at 4000 seconds. In principle an upper boundary should not be needed for the random walk model since particles should be prevented from moving too high by σ_w^2 becoming small. However, using a value of z_i based on the height at which the subgrid component of σ_w^2 becomes negligible, allowed particles to travel to a much greater height in the random walk model than in the L.E.S. model. This is possibly due to σ_w^2 at high levels being the result of waves which do not disperse particles in the L.E.S. model. For the single neutral simulation the boundary layer depth was limited by the domain depth (1200m), with the turbulence extending to the top of the domain. For this case the particles are not well mixed by 4000s.

Table 1 gives details of the seven L.E.S. runs used in this work. All runs used $z_0 =$ 0.1m. The number in the title of each run refers to the wind speed in the run, for example, LES7 is the L.E.S. model run which had a geostrophic wind speed of 7ms^{-1}. The corresponding random walk run is titled RW7.

The random walk particles' trajectories were recorded on a 50 × 500 grid, the coordinates being height and time respectively. The grid spacing in the vertical was $z_i/50$ and in the horizontal it was 8 seconds. The data are collected in the form of vertical profiles at 8 second intervals. All the particles were allowed to move for a total of 4000 seconds with no limit being put on their possible downwind distance. In the least convective case with a geostrophic wind speed of 20ms^{-1} the particles were able to travel up to 80km.

The time step Δt was taken as the minimum of the four expressions: (a) 0.05τ, (b) $0.1\sigma_w/|\partial\sigma_w^2/\partial z|$, (c) $0.05P\sigma_w/|-(\sigma_w^2 Q/\tau)+\phi|$, and (d) $0.05z_i/|w|$. Restriction (a) ensures that the particle velocity cannot change by a large fraction of σ_w due to $bd\xi$. Restriction (b) attempts to ensure that σ_w at the location of a particle cannot change by a large fraction due to changes in the particle's position while (c) prevents the velocity changing by a large fraction of σ_w due to adt. Restriction (d) prevents the particle moving by a large fraction of the boundary layer depth (note (b) may not be sufficient to prevent σ_w changing by a large fraction when $\partial\sigma_w^2/\partial z \simeq 0$ at the particle's location at the start of the time-step). Tests with constants smaller than those shown in these expressions (a) to (d) above made little difference to the model results, suggesting that our choice of Δt is sufficiently small to give time-step independent results.

It was found that reasonably stable dispersion statistics were obtained using 50000 particles in the L.E.S. but only 15000 were needed in the random walk model. The need for more particles in the L.E.S. is presumably a consequence of the fact that the particle motions in the L.E.S. are not independent.

4 Model results

Random walk simulations were performed for each of the seven L.E.S. stability categories and for four release heights (25m, 100m, 200m and 400m). The results are discussed in detail for two release heights, 100m and 400m, and for three stability categories, free convection (runs RW0 and LES0), moderate convection (runs RW7 and LES7), and neutral conditions (runs RW20N and LES20N). Because of the considerable uncertainty about the appropriate value of C_0, one of the main aims was to discover the value of C_0 which gives best results in comparison to the L.E.S. results and the Willis and Deardorff tank experiments. We start with the random walk and large eddy simulations of dispersion in free convective conditions. Many of these results are presented in terms of the non-dimensional travel time $X = w_* t/z_i$, but dimensional results are given too in order to make comparisons with the results obtained in other stabilities easier.

Figures 2a and 2b show the horizontally integrated concentration profiles from the random walk and L.E.S. models for the 100m release of the free convective run ($z_i/L = -\infty$). The profiles are normalised so that they equal unity when the material is well mixed in the vertical up to z_i. Each graph consists of four curves each one representing the particle concentration profile at a specified time after release. The models are seen to predict the same general dispersion evolution with a large surface concentration after 500s (corresponding to a non-dimensional time X of 0.6) and uniform mixing after 4000s ($X = 4.8$). The 1000s and 2000s curves in both graphs show the characteristic lift-off effect

where the horizontally integrated concentration increases near the top of the boundary layer. The L.E.S. model predicts a corresponding decrease near the surface which the random walk model does not show. The random walk results were obtained using a value of $C_0 = 2.0$ as used in previous convective boundary layer simulations (Luhar and Britter 1989; Weil 1989); using C_0 values from 2.0 to 6.0 gave results not very different from those shown in figure 2a although for the larger C_0 values there was less 'lift off' with the height of maximum concentration remaining at ground level for longer and with lower concentrations at the boundary layer top after 1000s.

Figures 2c and 2d show the RW0 and LES0 concentration curves for the 400m release with the random walk model using $C_0 = 2.0$. The models agree only on the very general features of the evolution of the dispersion. For example, by 500s after release the random walk model shows a much wider plume and a significantly greater ground level concentration than the L.E.S. model. The rate of dispersion of particles in the random walk model is proportional to the total $\overline{w^2}$ which was taken as the sum of a resolved and a subgrid term, as described above. However, except in the lowest 100m of the boundary layer where the L.E.S. model includes random increments in the particles' positions to represent subgrid turbulent motions, the L.E.S. results are based on trajectories calculated using only the resolved velocity field. The particles in the random walk model thus experience a greater velocity variance and disperse faster than those in the L.E.S. model. The contribution of the subgrid term to the total variance varies with stability and height but generally represents between 20% and 30% of the total. To investigate this, some experiments were done with the random walk model using only the resolved part of $\overline{w^2}$ (but with $\overline{w^3}$ and τ as before). For the 400m release with $C_0 = 2.0$, this gave better agreement with the L.E.S. although it still overestimated the plume width somewhat. In this case the ratio of resolved $\overline{w^2}$ to total $\overline{w^2}$ in the corresponding L.E.S. run (LES0) is approximately 60% at 100m and 80% at 400m. If the total $\overline{w^2}$ is used in the random walk model, it is possible, by using a much higher value of C_0 (5.0 or 6.0), to obtain a better correspondence between the two models than that shown in figures 2c and 2d, although this change in C_0 has only a small effect on the plume spread after 500s. $C_0 = 2.0$ is the only value able to give the enhanced ground level concentration shown by the L.E.S. model after 1000s, although even with this value it underestimates the enhancement. Taken together these results suggest that C_0 values of about 2.0 may be best for the 400m release, with the main observed discrepancy (the much wider plume in the random walk simulations) being partly explained by the neglect of the subgrid motions in the L.E.S. dispersion calculation.

Figure 3a shows the development of the mean particle height corresponding to figure 2. The models make almost identical predictions for the development of the mean height of the lower release but disagree on the higher release with the L.E.S. model predicting a marked dip in the average height at 1000s. Two other large eddy studies (Nieuwstadt and De Valk, 1987 and Van Haren and Nieuwstadt, 1989) predict a much shallower dip more consistent with the random walk results. In runs using a range of C_0 values from 2.0 to 6.0 a trend emerges of a decreasing peak in the curve for the 100m release and a shallowing of the dip for the 400m release height, i.e. the dispersion becomes more diffusion-like as expected. Figure 3b shows the corresponding standard deviation of the particle heights. Again increasing the C_0 values from 2.0 to 6.0 leads to a smoothing of the curves with the initial slope being constant and the subsequent peaks becoming less pronounced, though the minimum at 1200s in the 400m curve persists. For both release heights the random walk model shows faster dispersion of particles than the L.E.S., the difference in spread

at 500s being partly explained by the difference between the total $\overline{w^2}$ and the resolved $\overline{w^2}$, the latter being 60% and 80% of the former at 100m and 400m respectively.

The tank experiments of Willis and Deardorff (1976, 1978 and 1981) provide a second test of the models in free convective conditions. The three experiments of interest here involved the release of particles (neutrally buoyant oil droplets) at $0.067z_i$, $0.24z_i$ and $0.49z_i$. To allow closer comparison between the tank experiments and the random walk model, three additional random walk runs were performed using the L.E.S. profiles and particle release heights of 53m, 192m and 387m ($z_i = 762$m). The C_0 value used was the same as used in the comparisons presented above (i.e. 2.0).

Figures 4a, 4b and 4c show how the model and experimental mean particle heights compare. The agreement is excellent for the $0.067z_i$ and $0.49z_i$ release heights particularly in the first half of the simulations. For the $0.24z_i$ release the random walk curve appears to stay ahead of the tank data by a non-dimensional time interval (i.e. X interval) of about 0.3 but both predict the same general development of the dispersion. Also on the graphs are points from the L.E.S. simulations for similar release heights; only the mid-boundary layer L.E.S. release differs significantly from the tank and random walk results with the large dip in the mean height at $X = 1$. The random walk curves are very similar to those of Luhar and Britter (1989) and Weil (1989).

Figures 5a, 5b and 5c show the model and experimental vertical standard deviation. The general shapes of the $0.067z_i$ curve and data are the same but the random walk model predicts the faster dispersion; the L.E.S. data points support the experimental predictions at small times. In figure 5b for the $0.24z_i$ release, the initial slopes of the random walk model, the experimental data and the L.E.S. data are in agreement but the experiments then predict a slowing down in the dispersion process. Again the random walk model predicts the more rapid dispersion development. At this height the resolved $\overline{w^2}$ represents about 75% of the total $\overline{w^2}$. Figure 5c for the $0.49z_i$ release shows the random walk model and experiments to be in almost complete agreement on the rate and general structure of the dispersion. The L.E.S. data does not to show the maximum at $X \sim 1$ but the lack of data points may partly disguise this.

Figure 6 shows contours of the dimensionless cross-wind integrated particle concentration from the random walk runs corresponding to the Willis and Deardorff experiments. For the near surface release (figure 6a) the experiments (see Willis and Deardorff 1976) and random walk model both show an initial high ground level concentration which decreases relatively quickly as the material is transported to the top of the boundary layer. In common with Luhar and Britter (1989), the random walk model fails to show the concentration increasing away from the ground at X values between 0.5 and 1.0 as is observed in the experiments. The concentration gradient is however close to zero and much smaller than that obtained with $C_0 = 3.5$; it seems likely that a value a little less than 2.0 (which will cause less diffusion-like behaviour) would give the observed counter-gradient transport near the ground. For the $0.24z_i$ release (figure 6b and Willis and Deardorff 1978) the height of the concentration maximum initially descends to the ground. By $X = 2$ the height of maximum concentration has lifted off to the upper part of the boundary layer, but is rather higher in the random walk simulations than in the experiment. For the mid-boundary-layer release (figure 6c and Willis and Deardorff 1981) the correspondence is very good with both the spatial details of the concentration distribution and its mag-

nitude in agreement. Overall the comparisons with Willis and Deardorff tend to support the value $C_0 = 2$ adopted in previous studies and supported by the comparisons between the large-eddy and random walk simulations discussed above.

The moderately convective case (runs RW7 and LES7) will now be considered. Figures 7a and 7b show the concentration profiles for the 100m release using $C_0 = 2.0$. The models predict similar dispersion development with large surface concentrations after 500s and 1000s. Higher values of C_0 give a better correspondence between the ground level concentrations after 1000s. As before, this is probably at least partly due to the fact that only the resolved $\overline{w^2}$ contributes to the L.E.S. dispersion, although this is not confirmed by the standard deviation of particle heights (see figure 8b below) for which, with $C_0 = 2$, the random walk gives slightly smaller values than the L.E.S. A simple interpretation here seems difficult due to the strongly inhomogeneous nature of the turbulence (in particular the resolved turbulence) around the source height. By 2000s both models show enhanced high level concentrations (only very slightly in the random walk). At 4000s the random walk model predicts a uniform concentration but the L.E.S. profile still shows signs of lift-off with slightly lower concentrations at the surface than higher up. Higher C_0 values (5.0 or 6.0) suppress any enhanced high level concentrations (consistent with the more diffusive behaviour expected) and tend to slow down the random walk model too much so that even at 4000s the distribution still has a larger concentration in the lower half of the boundary layer than in the upper half. On balance $C_0 = 2.0$ gives best results.

Figures 7c and 7d are the corresponding profiles for the 400m release with the random walk model using $C_0 = 3.5$, the value we judged to give best results. The models show similar dispersion development and give a uniform distribution at 4000s. Higher values of C_0 again lead to concentration profiles that match slightly better those of the L.E.S. model at small times (for example the maximum concentration agrees better). Note however that σ_z (see figure 8b below) is about right for $C_0 = 3.5$. Using the parameters of this run in the extension of Rodean's theory given above (equation (6)) leads to a value of $C_0 = 8.2$ at 100m and 9.3 at 400m. These values are not supported by the comparisons presented here. This might be because the value of C_0 does not depend on surface layer characteristics. Also the concept of an eddy diffusivity (which forms a central part of Rodean's argument) is less valid in this situation because of the larger turbulent length scales which occur (relative to the neutral case).

Figure 8a shows the mean plume heights corresponding to figure 7. Again the models agree on the development of the lower release but the L.E.S. predicts a significantly lower average height for the higher release. $C_0 = 2.0$ was by far the best value for the 100m release, larger values reduced the gradient of the curve quite significantly. The value of C_0 did not have a large effect on the 400m curve - $C_0 = 3.5$ was just slightly better than other values in the range 2.0 to 6.0. Figure 8b shows the standard deviation; here the model curves match fairly well at small times although the L.E.S. model does show slightly faster development for the 100m release and slightly slower development for the 400m release. The resolved $\overline{w^2}$ at 400m is 60% of the total leading to the expectation that the random walk plume would grow faster in relation to the L.E.S. than it does and that the best value of C_0 may be a little less than 3.5.

Figures 9 show the concentration profiles for the neutral runs RW20N and LES20N using $C_0 = 8.0$ in the random walk model. Figures 9a and 9b show the profiles for the

100m release while figures 9c and 9d show those for the 400m release. The L.E.S. profiles are slightly unreliable as some of the slow moving particles near the ground were lost from the three dimensional grid of boxes in which the particle positions were recorded; this grid moved downwind centred on the particles' centre of mass. The result of this is that the ground level concentrations in particular may be less than expected. We have normalised these curves so that the area under them is unity despite the loss of particles. For these simulations it was found that agreement between the models could only be obtained using a much larger value of C_0 than in the convective cases. The value 8.0 was found to give reasonable agreement for both release heights, consistent with the range 5 to 10 given by Sawford and Guest (1988). Random walk simulations with $C_0 = 6.0$ show faster plume growth than the L.E.S., but this may be due to the lack of subgrid influence on the L.E.S. dispersion ($\overline{w^2}$ resolved is 77% of the total at 400m). Hence Rodean's value of 5.7 is compatible with the results. Lower values (4.0 or less) allowed the random walk model to diffuse the particles too quickly while higher values (10.0 to 12.0) slow down the diffusion too much. The roughly uniform distribution obtained in the random walk model at 4000s for the 400m release is not mirrored by the L.E.S. model, probably because of the loss of particles at large times as mentioned above.

The evolution of particle mean height and standard deviation showed the same dependence on C_0 as in the other runs. Low values allowed too rapid a diffusion while high values slowed it down too much. Figure 10 shows the mean and standard deviation of the particle heights corresponding to figure 9. Figure 10a shows good agreement between the particles' mean height from the two models. The mismatch at large times shown in figure 10b for the standard deviation is significant and could not be much reduced even with very large C_0 values (around 12.0); it is probably associated with the loss of particles in the L.E.S. model.

The comparisons of the results of the random walk and L.E.S. model runs for three stability conditions and two release heights, described above, illustrate the more general results shown in figure 11. These figures give our assessment of the best value of C_0 for the run and release height in question. Generally, the random walk model is able to give good correspondence with the L.E.S. results for a range of values from 2.0 to 5.0 in convective conditions and from 7.0 to 10.0 in neutral conditions. This is consistent with previous results.

5 Summary

Considering the comparisons over the range of stabilities and release heights, it seems that the random walk model is able to reproduce many aspects of the L.E.S. and experimental results. It proved difficult to identify a single best value of C_0 for each stability category and release height, due partly to the complication caused by the fact that dispersion in the L.E.S. is not affected by subgrid motions above the lowest 100m. Our best estimates of C_0 show no clear relation between the optimum value of C_0 and release height, but the results do show a clear dependence of C_0 on stability. This dependence is consistent with the results of previous work which indicate that a much larger value is appropriate in neutral conditions than in convective conditions. A straightforward extension of Rodean's (1991)

argument to account for stability effects does not appear to give the correct behaviour for C_0.

References

Carruthers, D. J., Holroyd, R. J., Hunt, J. C. R., Weng, W.-S., Robins, A. G., Apsley, D. D., Smith, F. B., Thomson, D. J. and Hudson, B. (1992) UK Atmospheric Dispersion Modelling System. Air pollution modeling and its application IX, Plenum Press.

Lamb, R. G. (1978) Numerical simulation of dispersion from an elevated point source in the convective boundary layer. *Atmos. Environ.*, **12**, 1297-1304.

Legg, B. J. and Raupach, M. R. (1982) Markov simulation of vertical dispersion in inhomogeneous flows. *Boundary-Layer Meteorol.*, **24**, 3-13.

Luhar, A. K. and Britter, R. E. (1989) A random walk model for dispersion in inhomogeneous turbulence in a convective boundary layer. *Atmos. Environ.*, **23**, 1911-1924.

Mason, P. J. (1992) Large-eddy simulation of dispersion in convective boundary layers with wind shear. *Atmos. Environ.*, **26A**, 1561-1572.

Nieuwstadt, F. T. M. and De Valk, J. P. J. M. M. (1987) Buoyant and non-buoyant plume dispersion in the atmospheric boundary layer. *Atmos. Environ.*, **21**, 2573-2587.

Rodean, H. C. (1991) The universal constant for the Lagrangian structure function. *Phys. Fluids A***3**, 1479-1480.

Sawford, B. L. and Guest, F. M. (1988) Uniqueness and universality of Lagrangian stochastic models of turbulent dispersion. Eighth Symposium on Turbulence and Diffusion, American Meteorological Society, Boston.

Thomson, D. J. (1987) Criteria for the selection of the stochastic models of particle trajectories in turbulent flows. *J. Fluid Mech.*, **180**, 529-556.

Van Dop, H., Nieuwstadt, F. T. M. and Hunt, J. C. R. (1985) Random walk models for particle displacements in inhomogeneous unsteady turbulent flows. *Phys. Fluids*, **28**, 1639-1653.

Van Haren, L. and Nieuwstadt, F. T. M. (1989) The behaviour of passive and buoyant plumes in a convective boundary layer, as simulated with a large-eddy model. *J. Appl. Met.*, **28**, 818-832.

Weil, J. C. (1989) Stochastic modeling of dispersion in the convective boundary layer. Air pollution modeling and its application VII, Plenum Press.

Willis, G. E. and Deardorff, J. W. (1976) A laboratory model of diffusion into the

convective planetary boundary layer. *Q. J. R. Meteorol. Soc.*, **102**, 427-445.

Willis, G. E. and Deardorff, J. W. (1978) A laboratory study of diffusion from an elevated source within a modelled convective planetary boundary layer. *Atmos. Environ.*, **12**, 1305-1311.

Willis, G. E. and Deardorff, J. W. (1981) A laboratory study of dispersion from a source in the middle of a the convective mixed layer. *Atmos. Environ.*, **15**, 109-117.

Table 1

	z_i	Z_c	u_*	w_*	L	z_i/L
LES0	762	790	0.00	0.92	-0.0	$-\infty$
LES2	820	885	0.17	0.96	-13	-68
LES4	876	900	0.29	0.97	-59	-15
LES7	858	910	0.38	0.97	-132	-7
LES10	1086	970	0.55	0.99	-420	-2
LES20	934	940	0.85	0.98	-1544	-0.6
LES20N	1200	1104	0.72	0.00	∞	0.0

Table 1: Parameters of L.E.S. Model Runs.

Figure Captions

Figure 1: Probability density function for vertical velocities, P(z,w), for heights of 100m and 400m in a convective boundary layer and in a neutral boundary layer as given by equation (2) using $\overline{w^2}$ and $\overline{w^3}$ from the large-eddy simulations of Mason (1992). The dashed/dotted line and the dashed line show the free convective 100m and 400m curves respectively while the pecked line and the dotted line show the neutral 100m and 400m results.

Figure 2: Vertical profiles of crosswind integrated concentration for free convective runs RW0 and LES0. The dashed line, the dotted line, the pecked line and the dashed/dotted line give results for 500s, 1000s, 2000s and 4000s (i.e. $X = 0.6$, 1.2, 2.4 and 4.8) respectively. (a) Random walk 100m release. (b) Large eddy simulation 100m release. (c) Random walk 400m release. (d) Large eddy simulation 400m release.

Figure 3: Statistics for free convective runs RW0 and LES0. The dotted line and the pecked line show the random walk results for the 100m and 400m releases respectively, while the crosses and squares show the large eddy results for the same release heights. (a) Mean height of particles. (b) Standard deviation of particle heights.

Figure 4: Mean height of particles for the free convective random walk and large-eddy simulations and the Willis and Deardorff experiments. The solid line shows the L.E.S.

data, the dotted line the random walk results and the circles the Willis and Deardorff observations. The L.E.S. release heights were not chosen to match the experiments and so differ a little from the values in the random walk simulations and in the experiments. (a) Release at $z/z_i = 0.067$. (b) Release at $z/z_i = 0.24$. (c) Release at $z/z_i = 0.49$.

Figure 5: Standard deviations of particle heights for the free convective random walk and large-eddy simulations and the Willis and Deardorff experiments. The various lines and symbols are as in figure 4. The L.E.S. release heights were not chosen to match the experiments and so differ a little from the values in the random walk simulations and in the experiments. (a) Release at $z/z_i = 0.067$. (b) Release at $z/z_i = 0.24$. (c) Release at $z/z_i = 0.49$.

Figure 6: Contours of crosswind integrated concentration from the free convective random walk simulations. (a) Release at $z/z_i = 0.067$. (b) Release at $z/z_i = 0.24$. (c) Release at $z/z_i = 0.49$.

Figure 7: Vertical profiles of crosswind integrated concentration for moderately convective runs RW7 and LES7. The various lines and symbols are as in figure 2. (a) Random walk 100m release. (b) Large eddy simulation 100m release. (c) Random walk 400m release. (d) Large eddy simulation 400m release.

Figure 8: Statistics for moderately convective runs RW7 and LES7. The various lines and symbols are as in figure 3. (a) Mean height of particles. (b) Standard deviation of particle heights.

Figure 9: Vertical profiles of crosswind integrated concentration for neutral runs RW20N and LES20N. The various lines and symbols are as in figure 2. (a) Random walk 100m release. (b) Large eddy simulation 100m release. (c) Random walk 400m release. (d) Large eddy simulation 400m release.

Figure 10: Statistics for neutral runs RW20N and LES20N. The various lines and symbols are as in figure 3. (a) Mean height of particles. (b) Standard deviation of particle heights.

Figure 11: Best estimates of the optimum value of C_0 in the random walk model for each of the various runs. Circles, plus signs, crosses and squares indicate values for the 25m, 100m, 200m and 400m releases respectively.

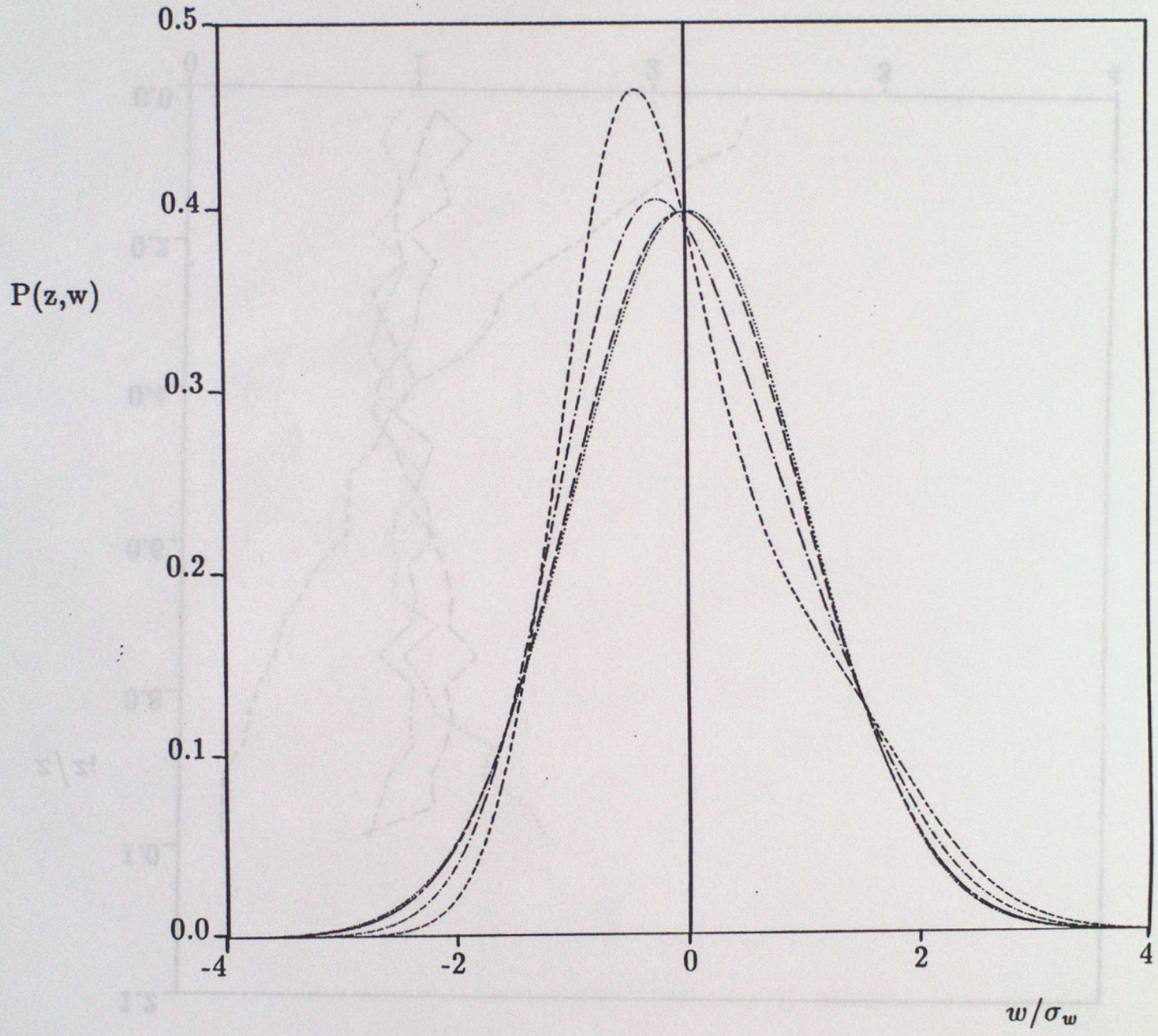

Figure 1

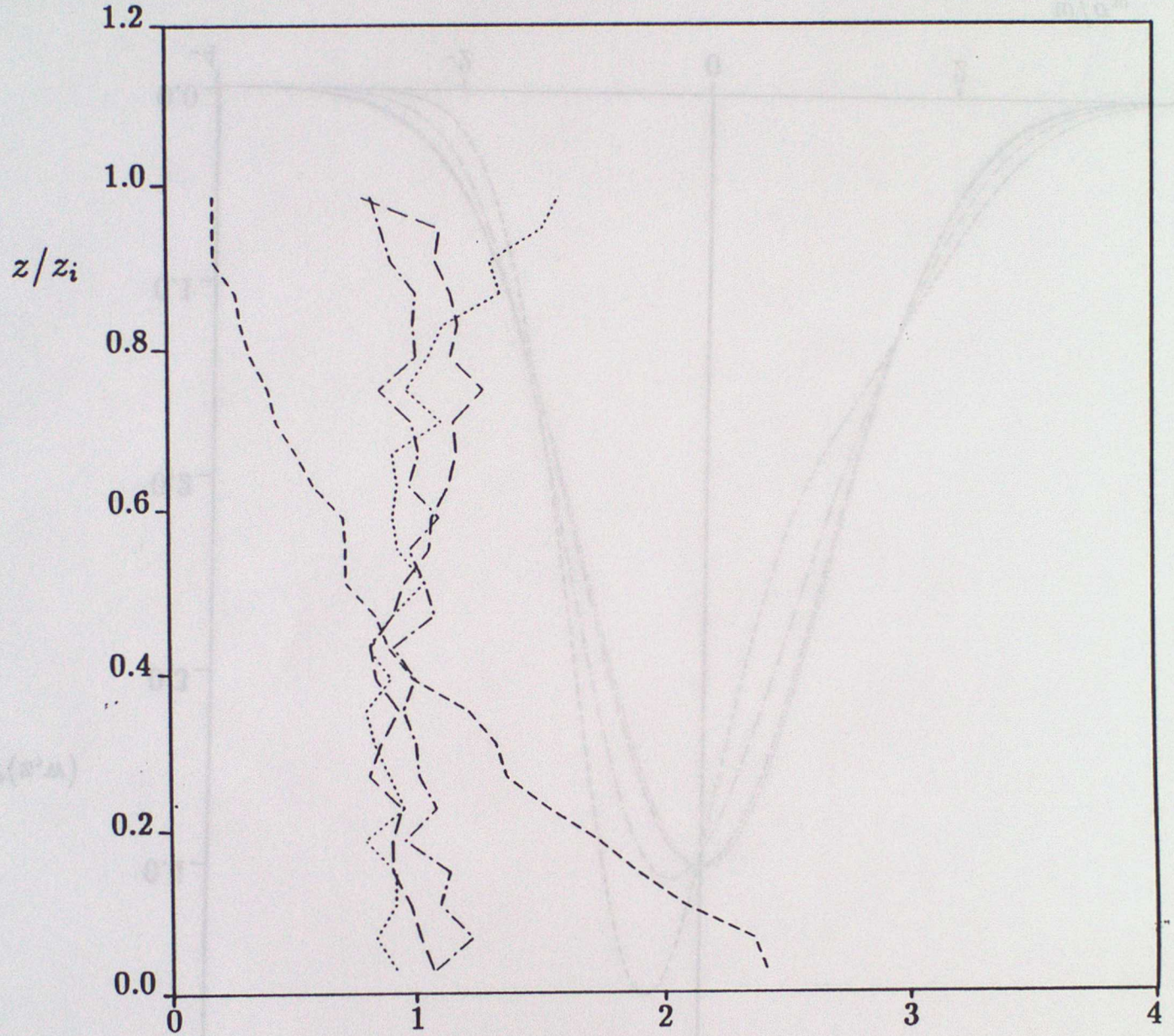

Figure 2a

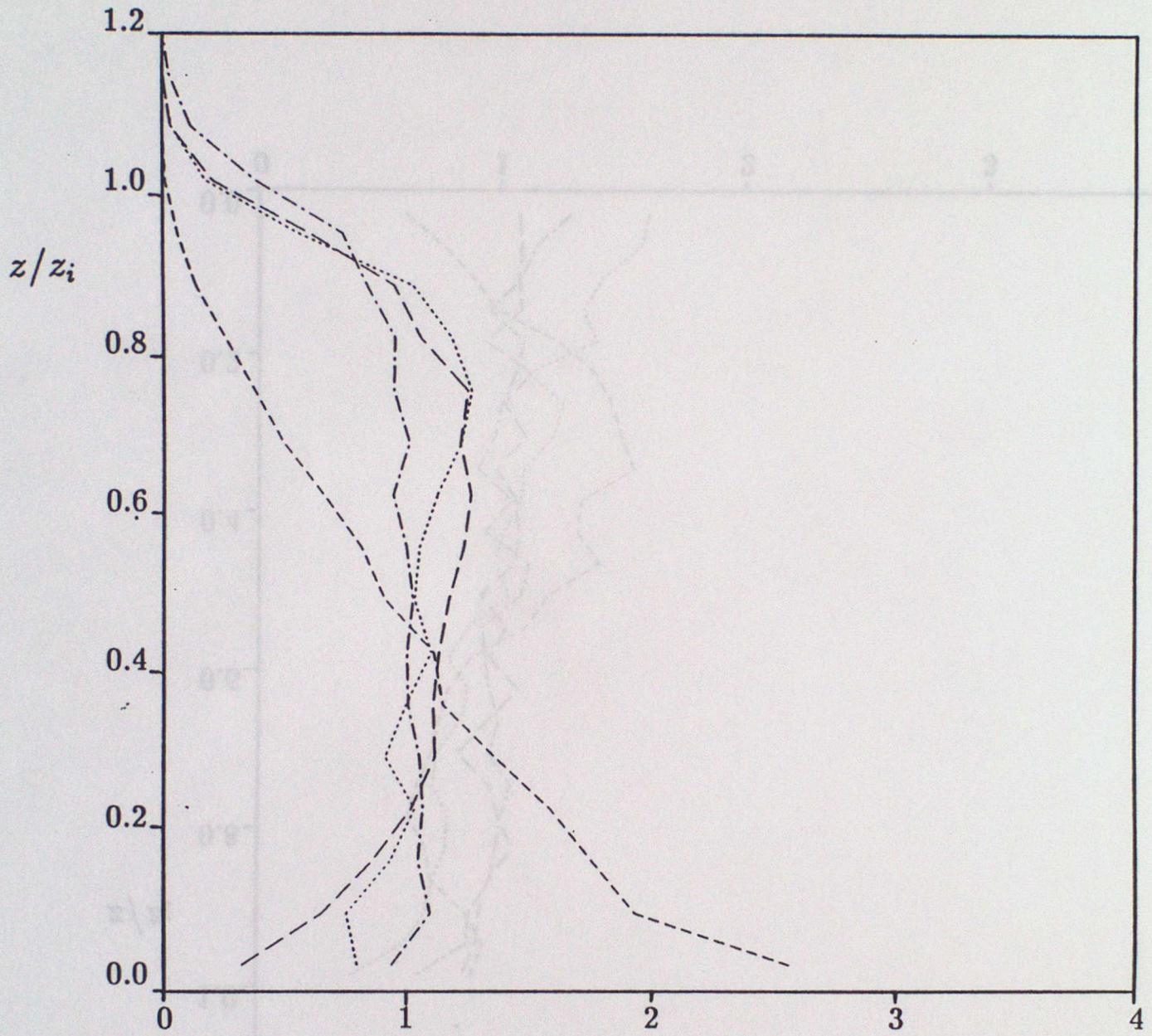

Figure 26

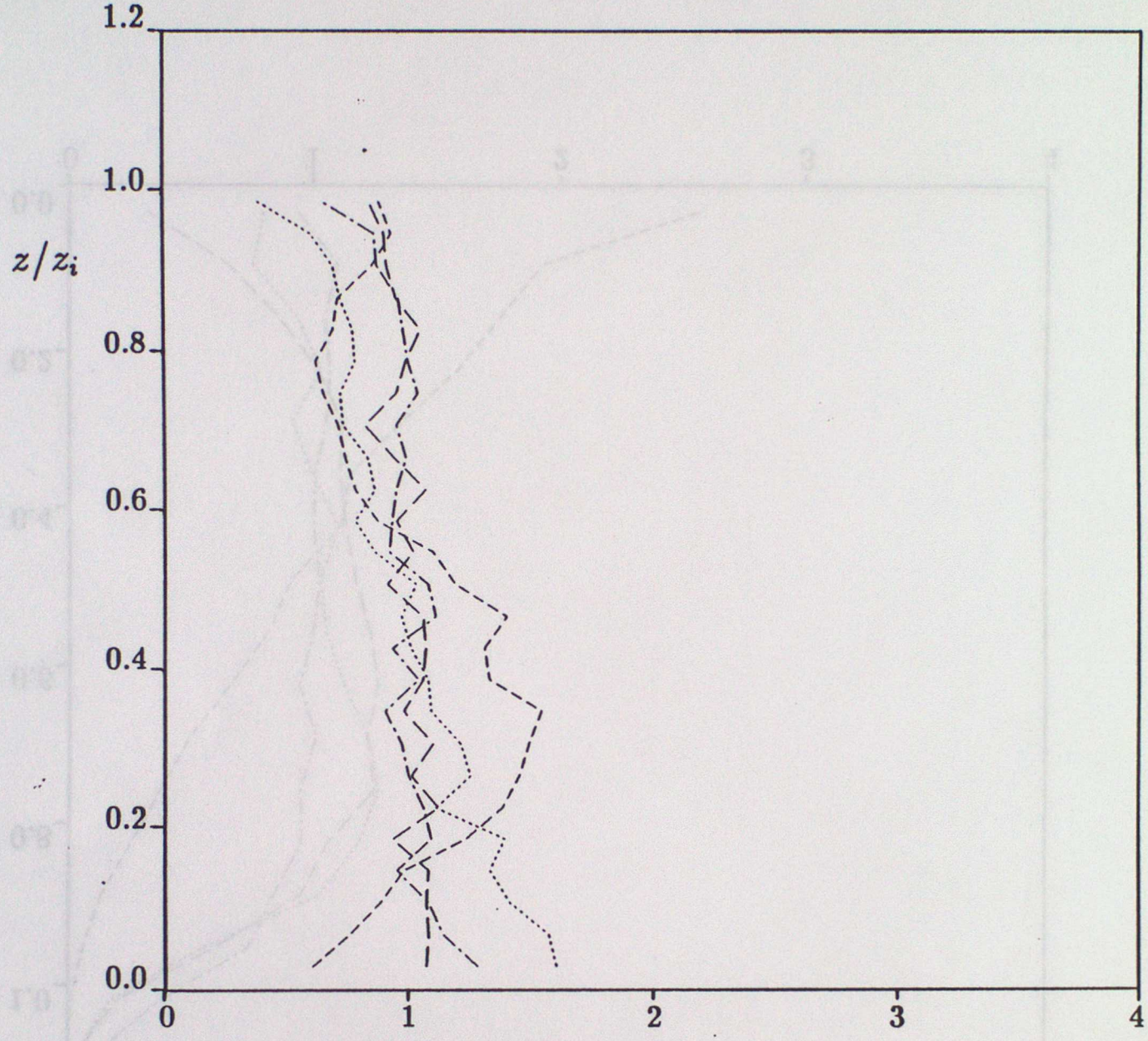

Figure 2c

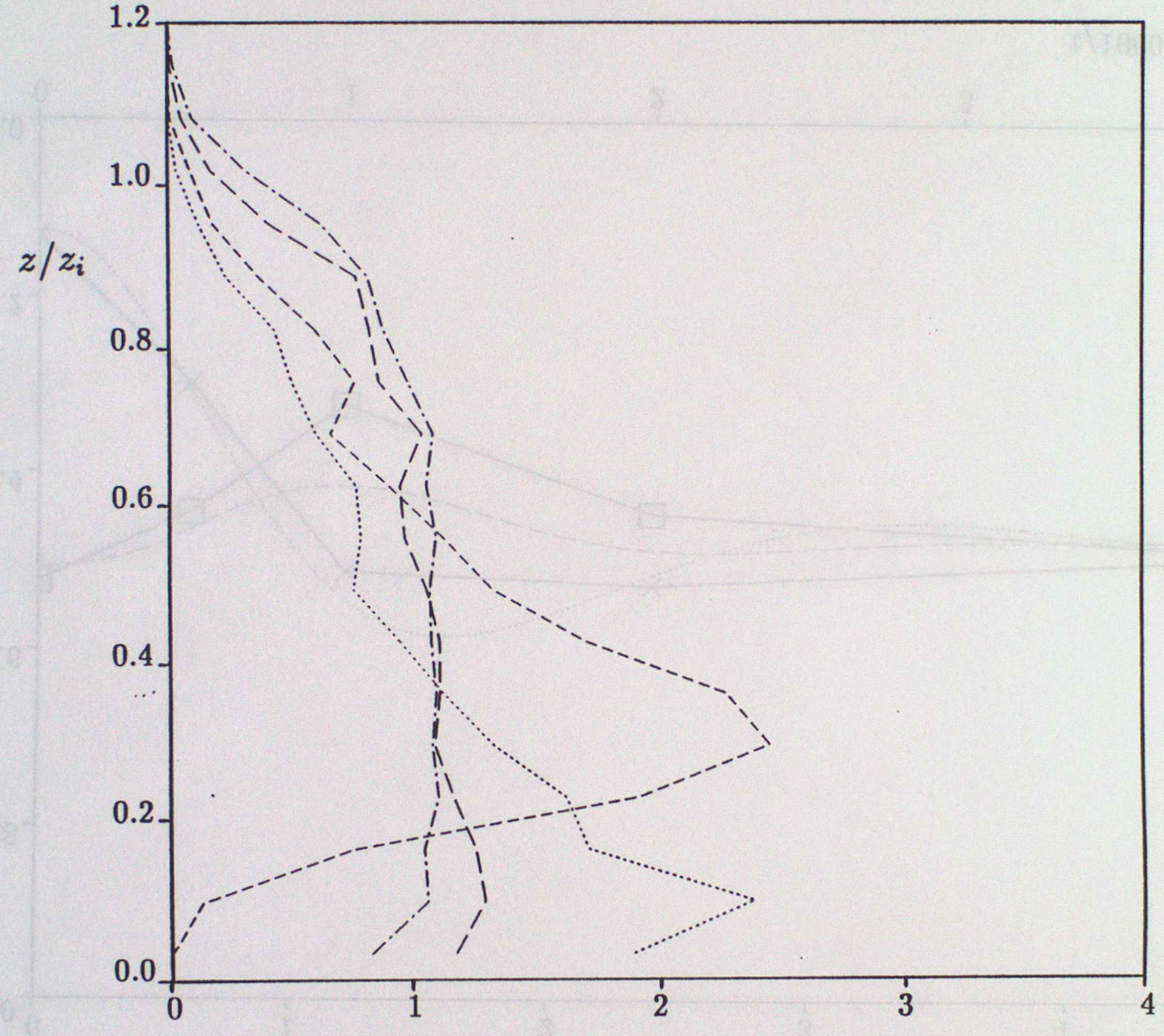

Figure 2d

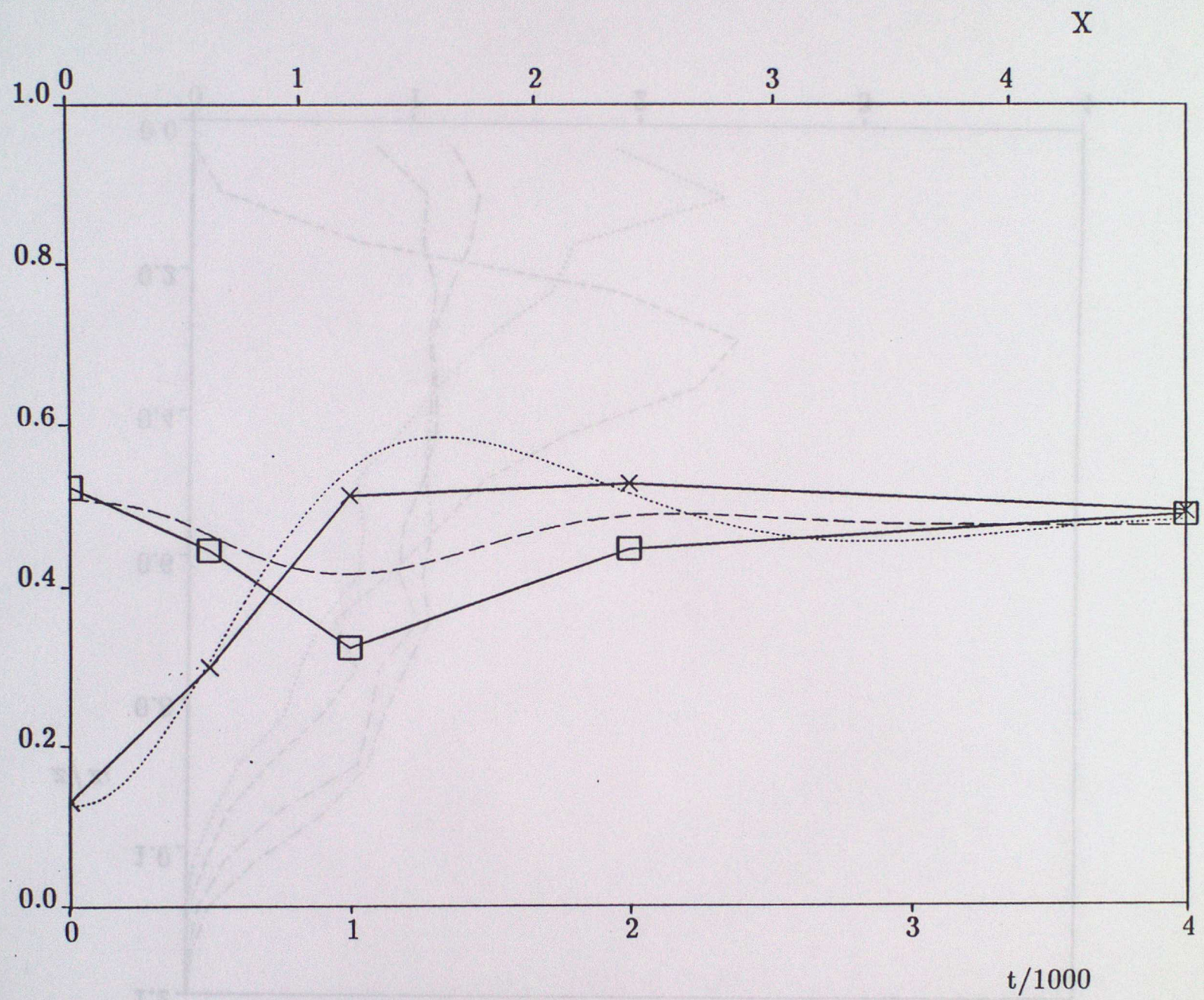

Figure 3a

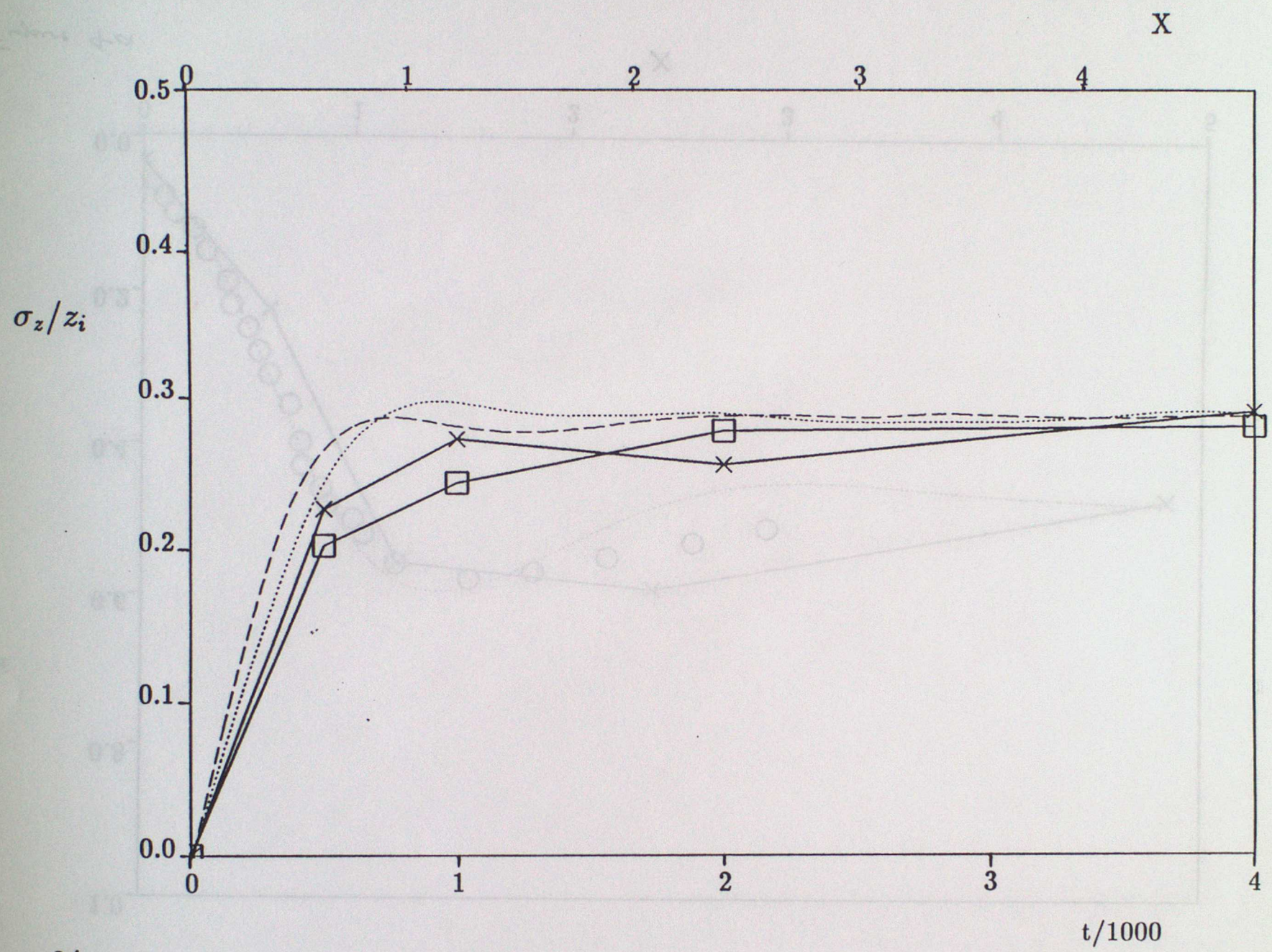

Figure 36

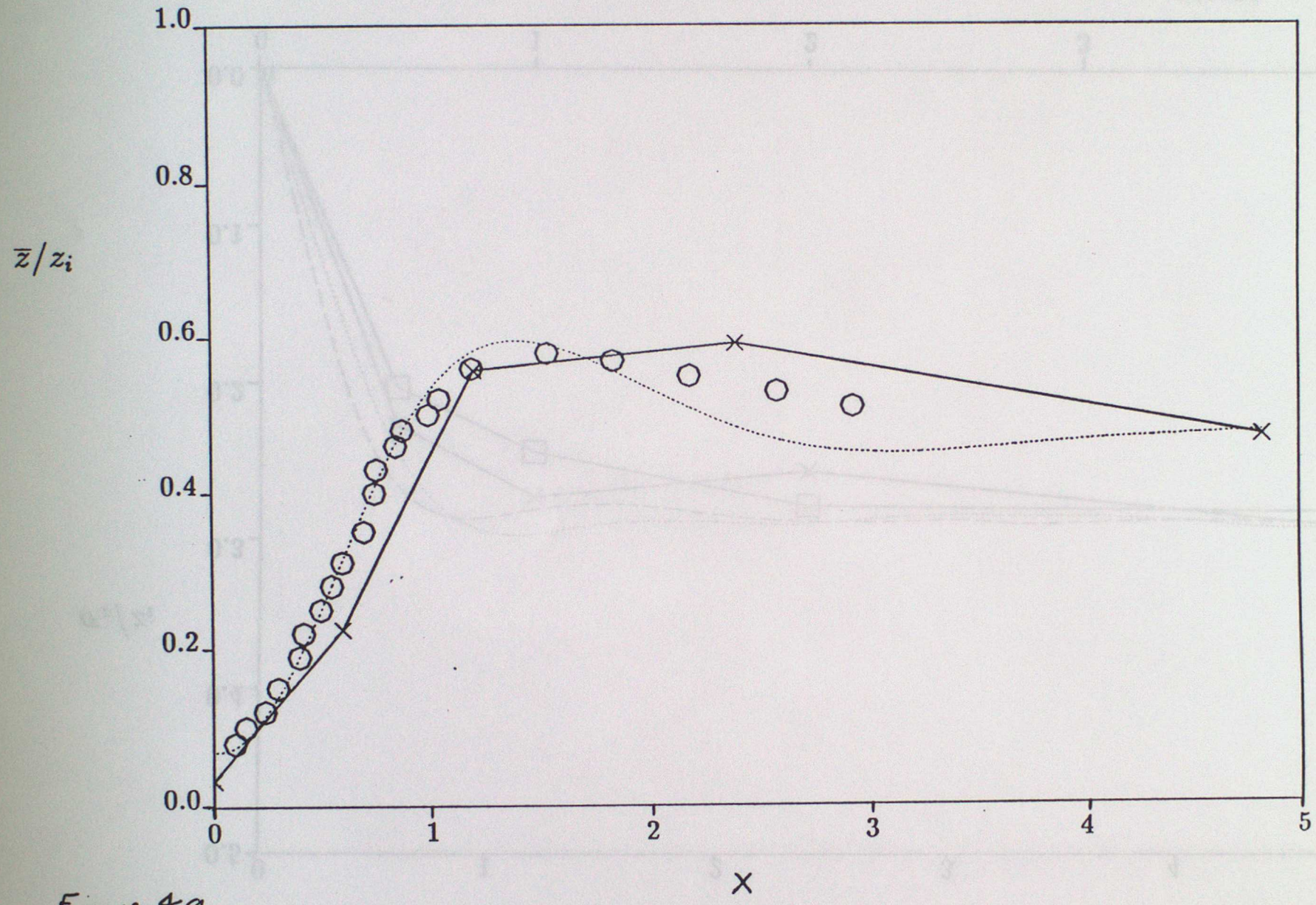

Figure 4a

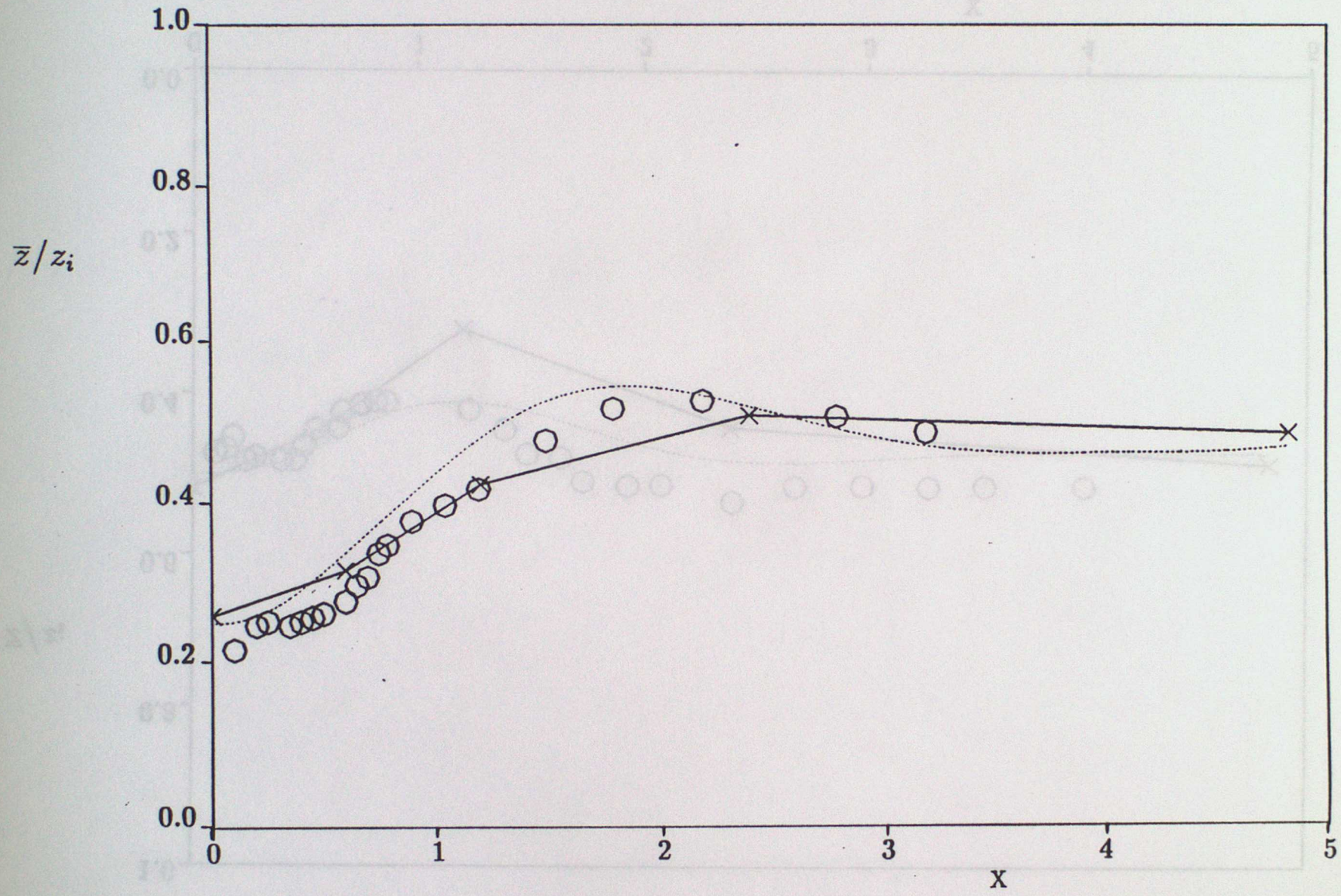

Figure 4b

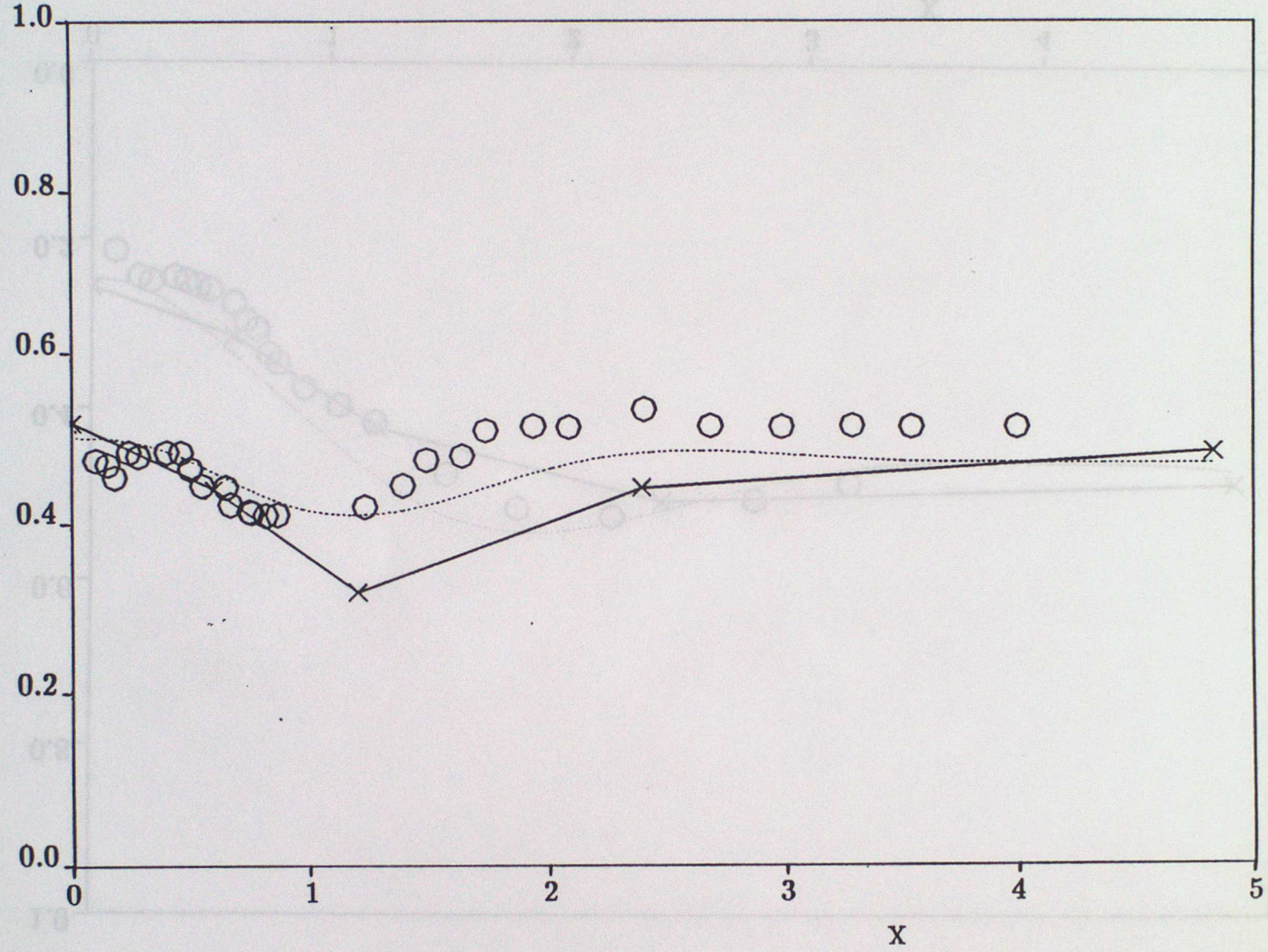

Figure 4c

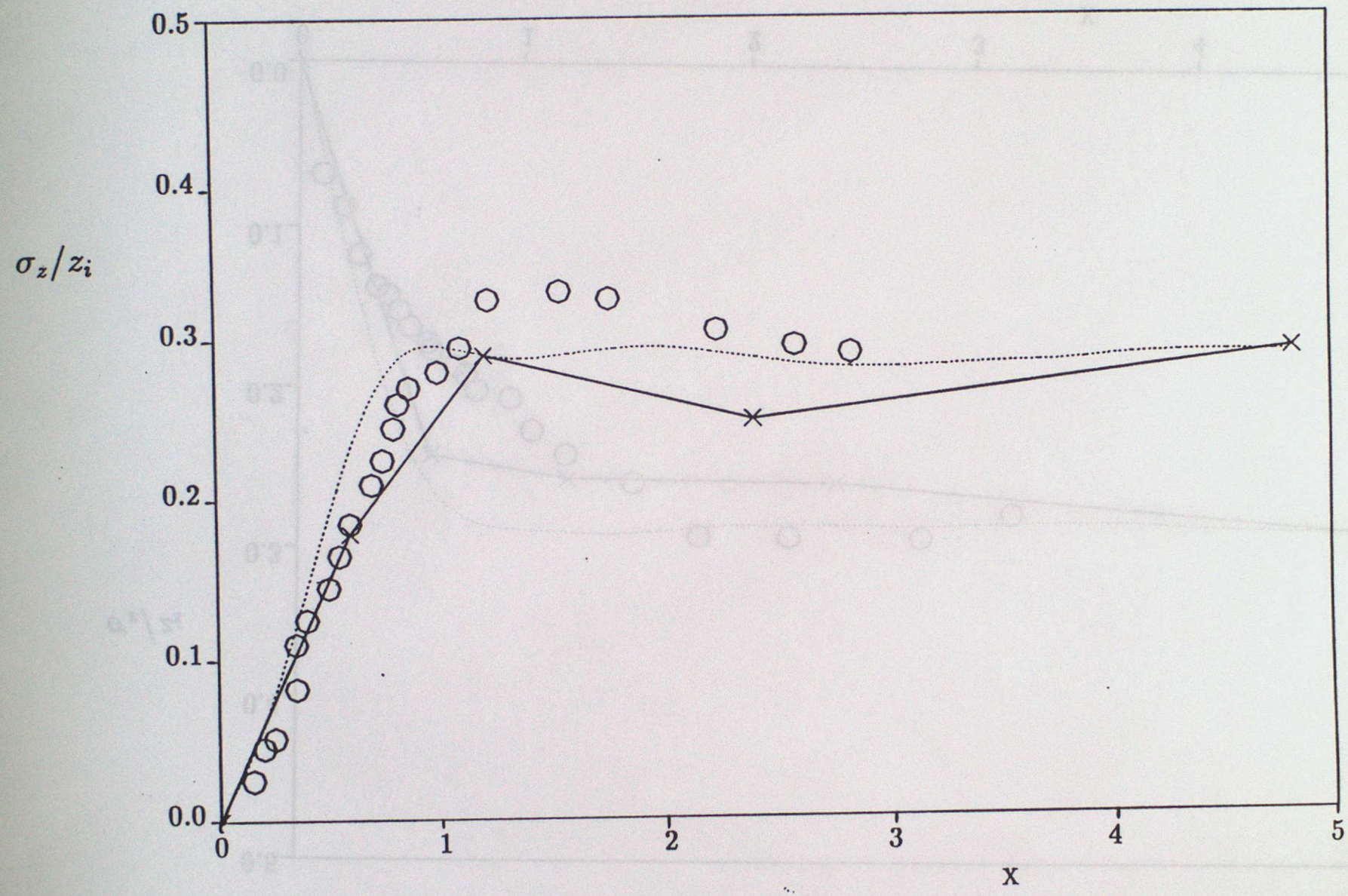

Figure 5a

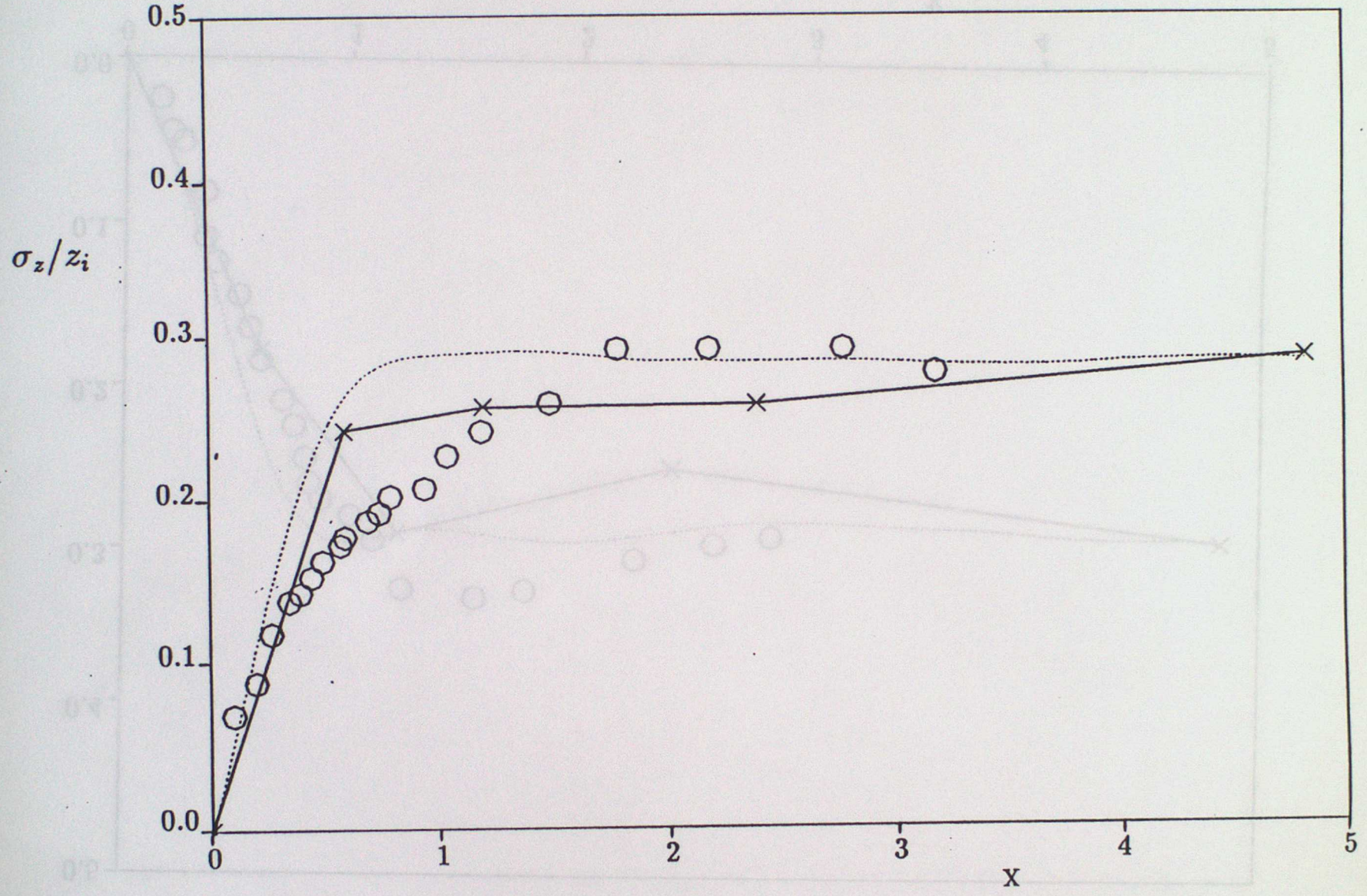

Figure 5b

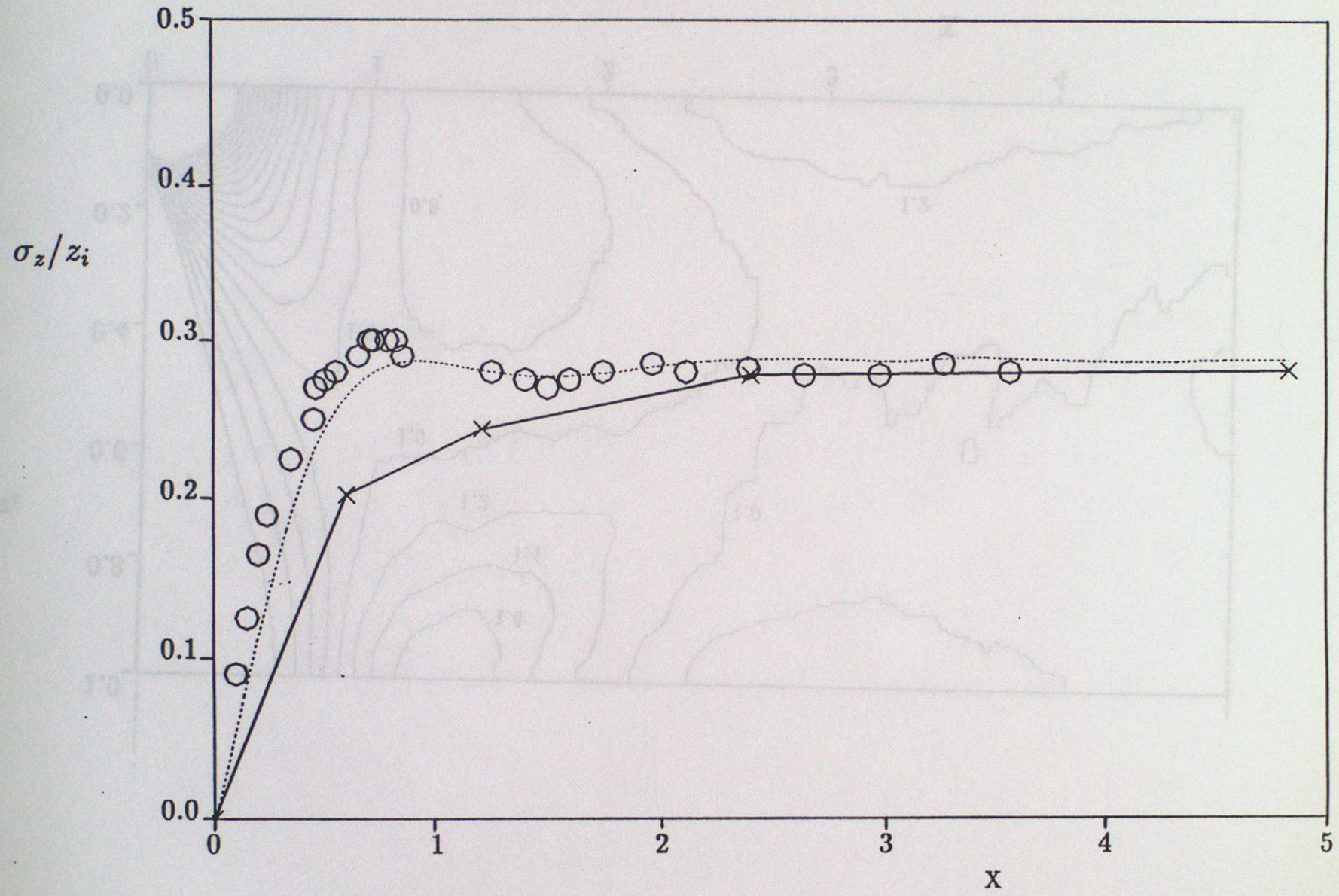

Figure 5c

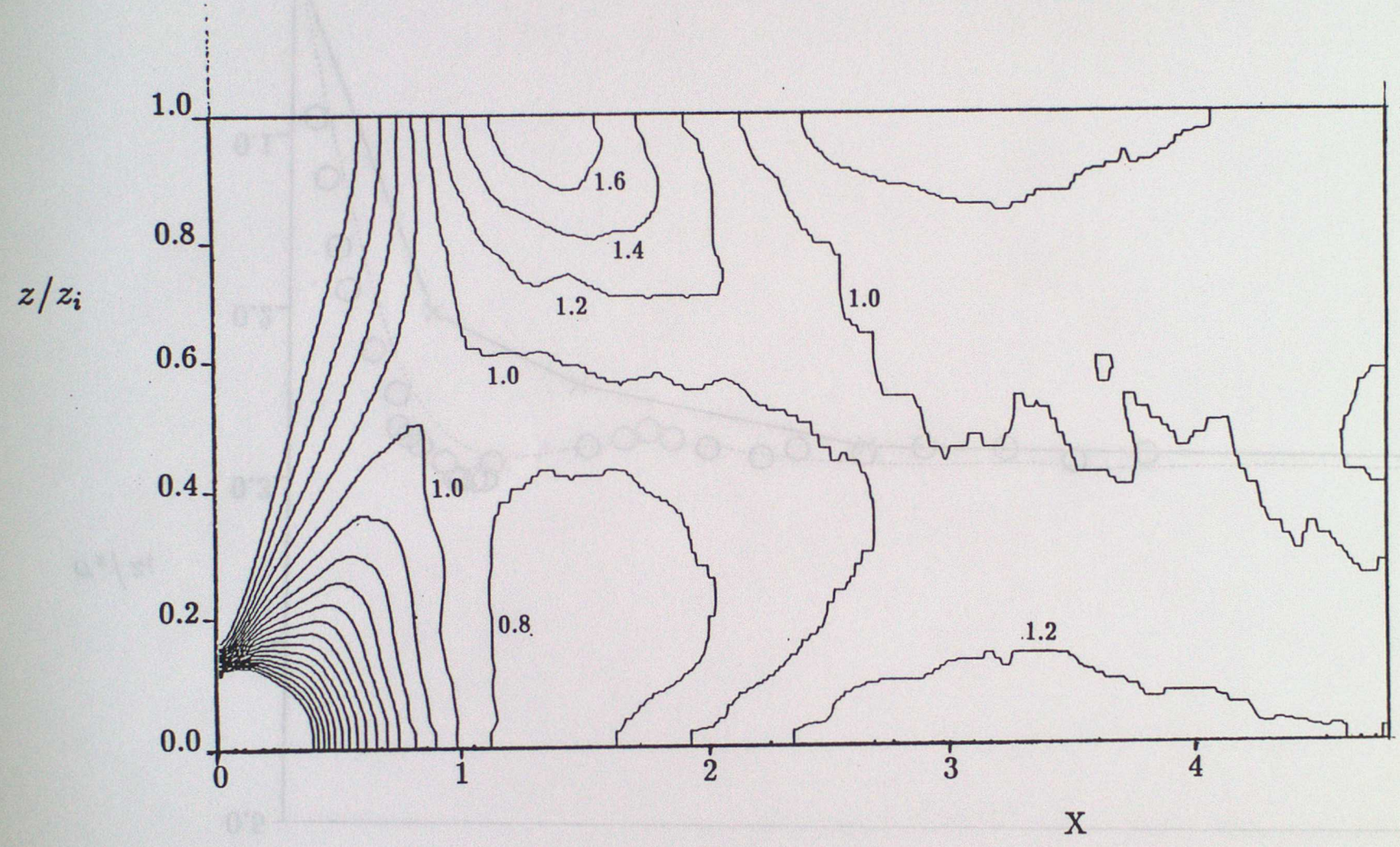

Figure 6a

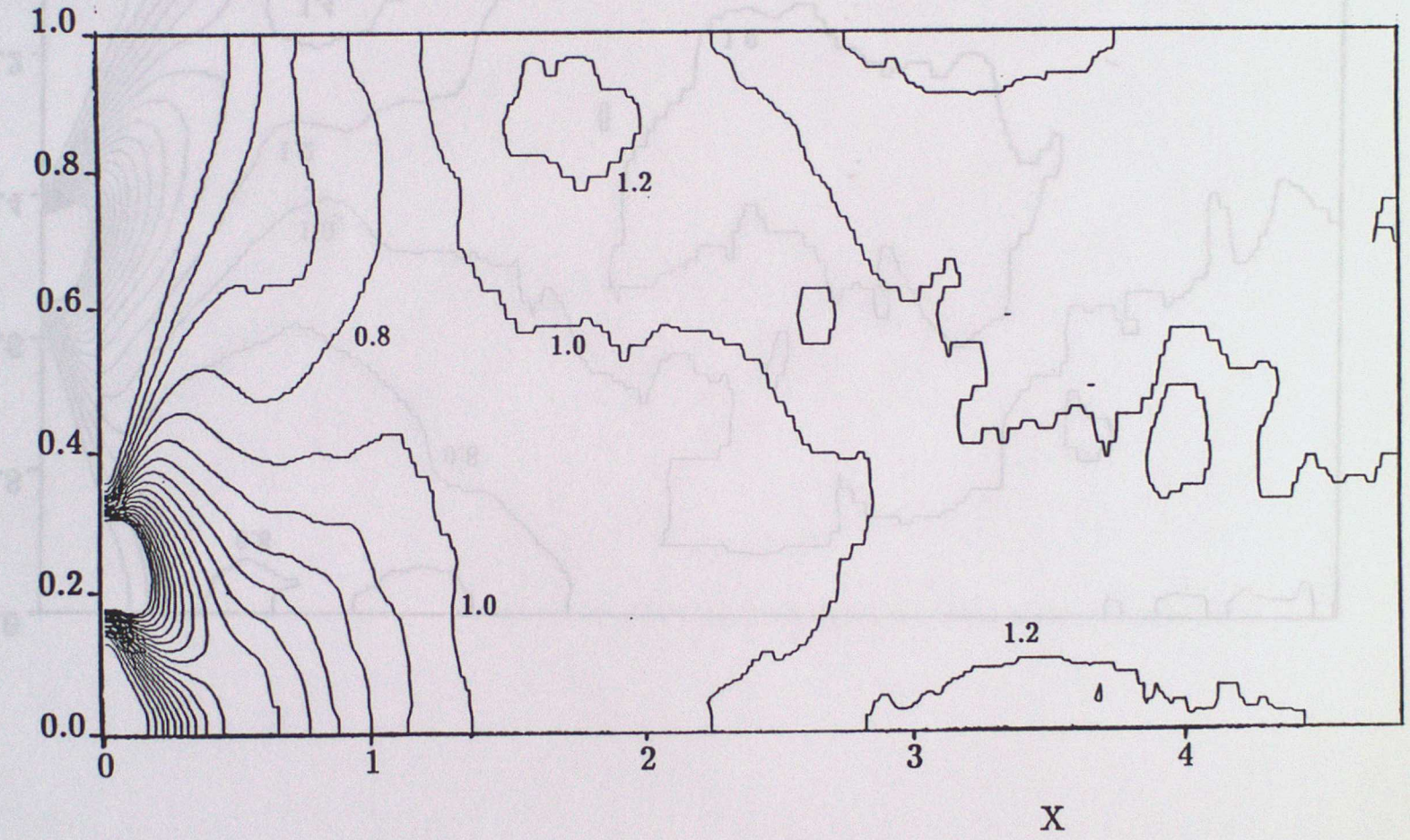

Figure 66

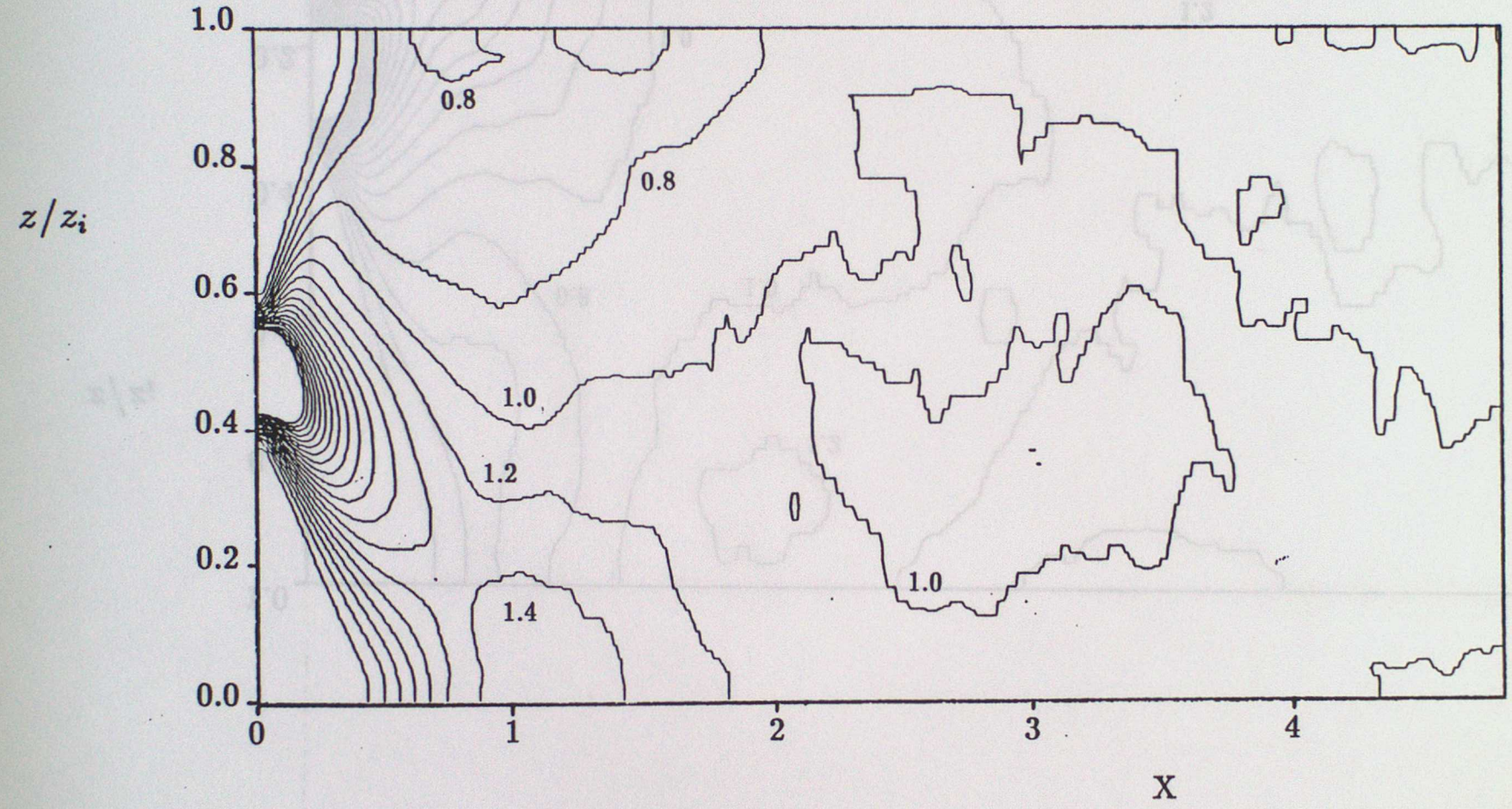

Figure 6c

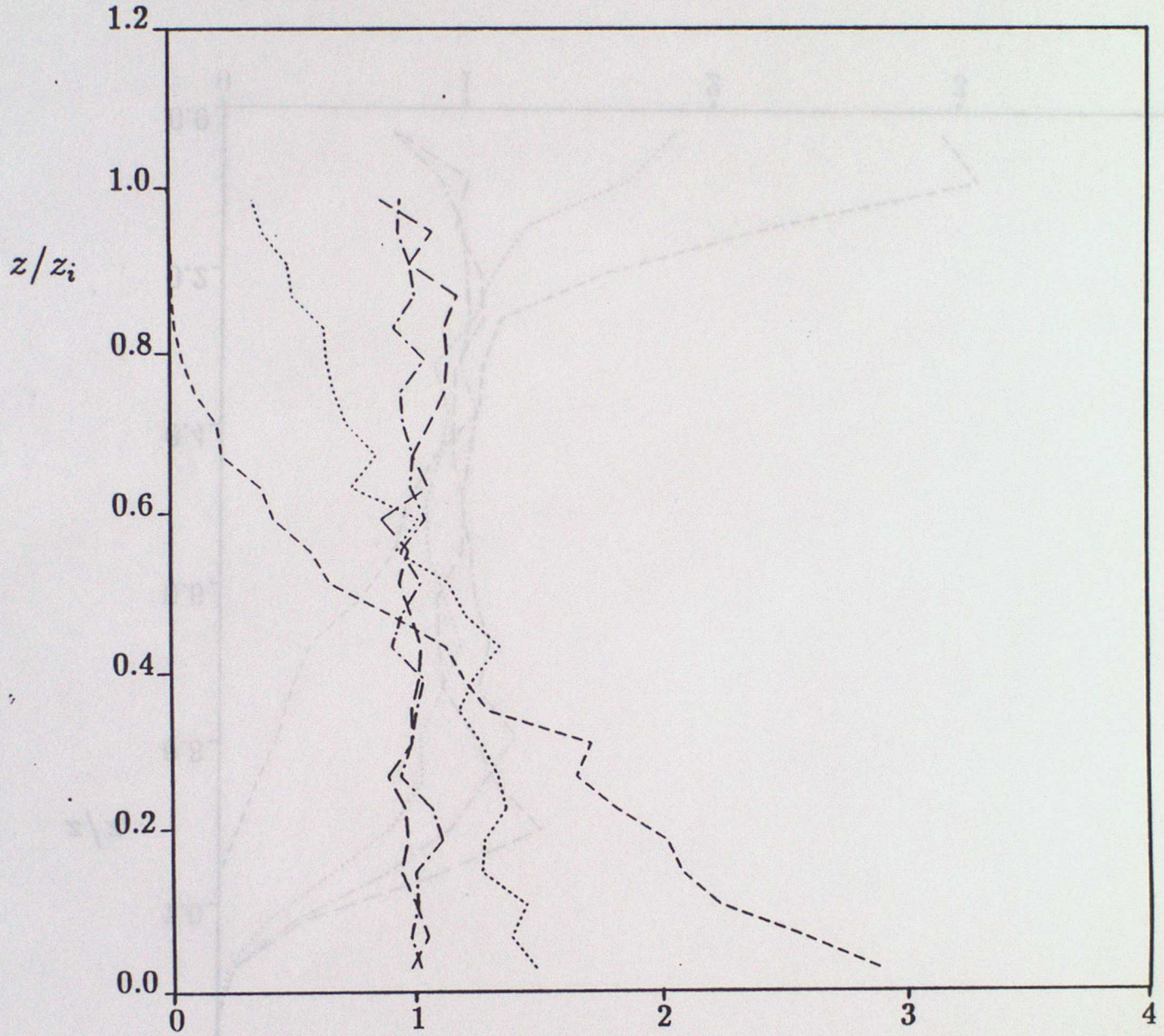

Figure 7a

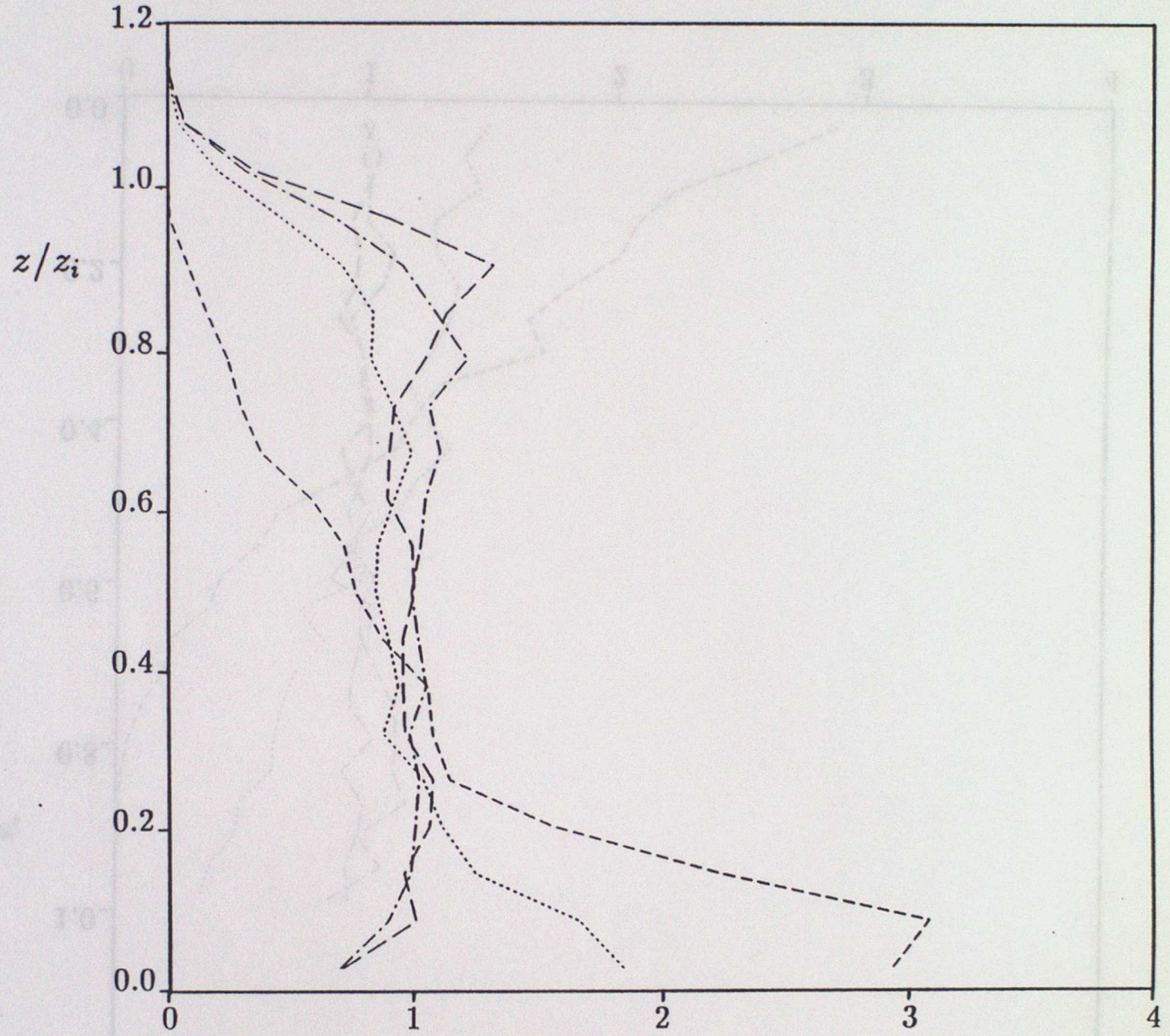

Figure 7b

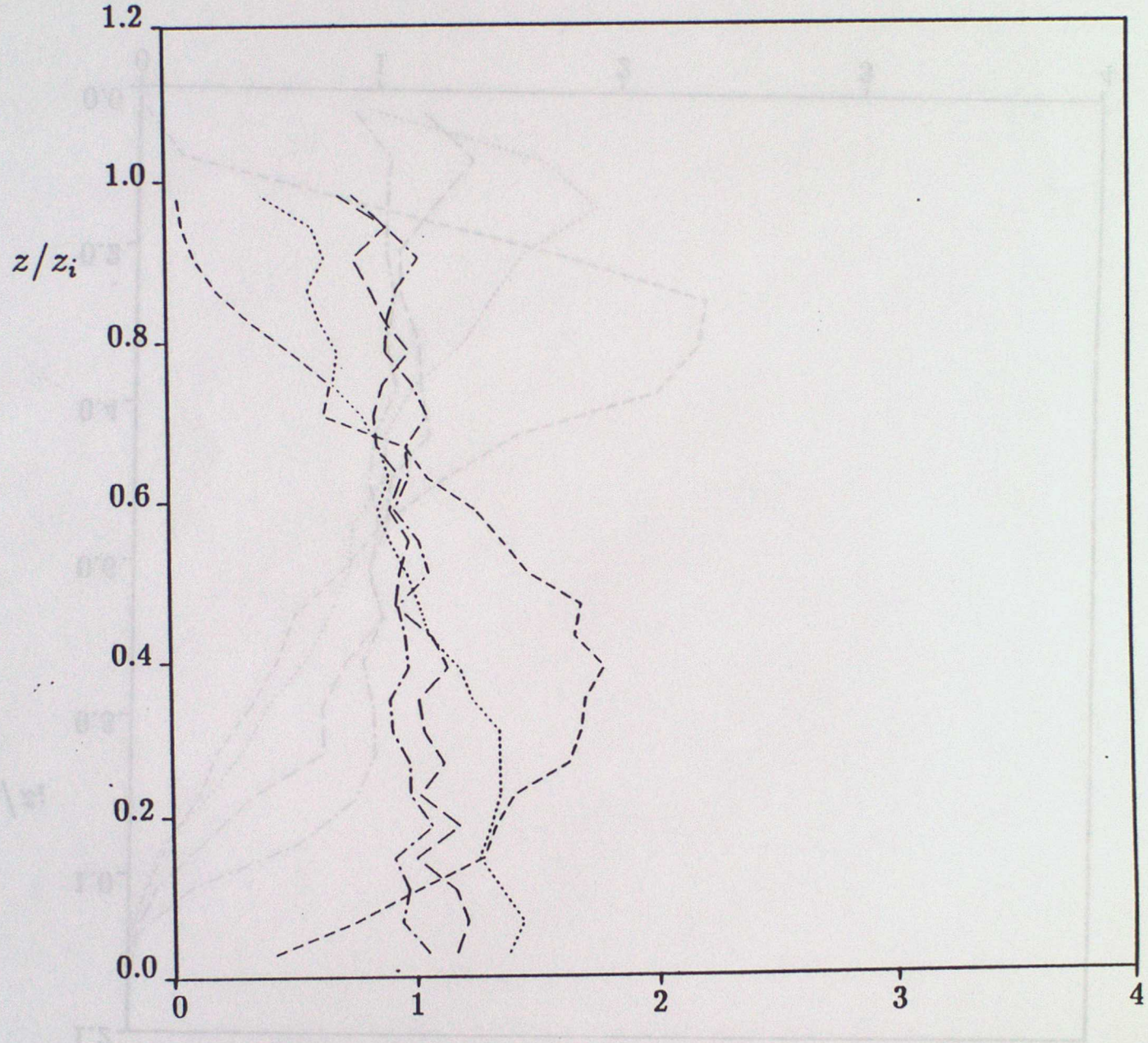

Figure 7c

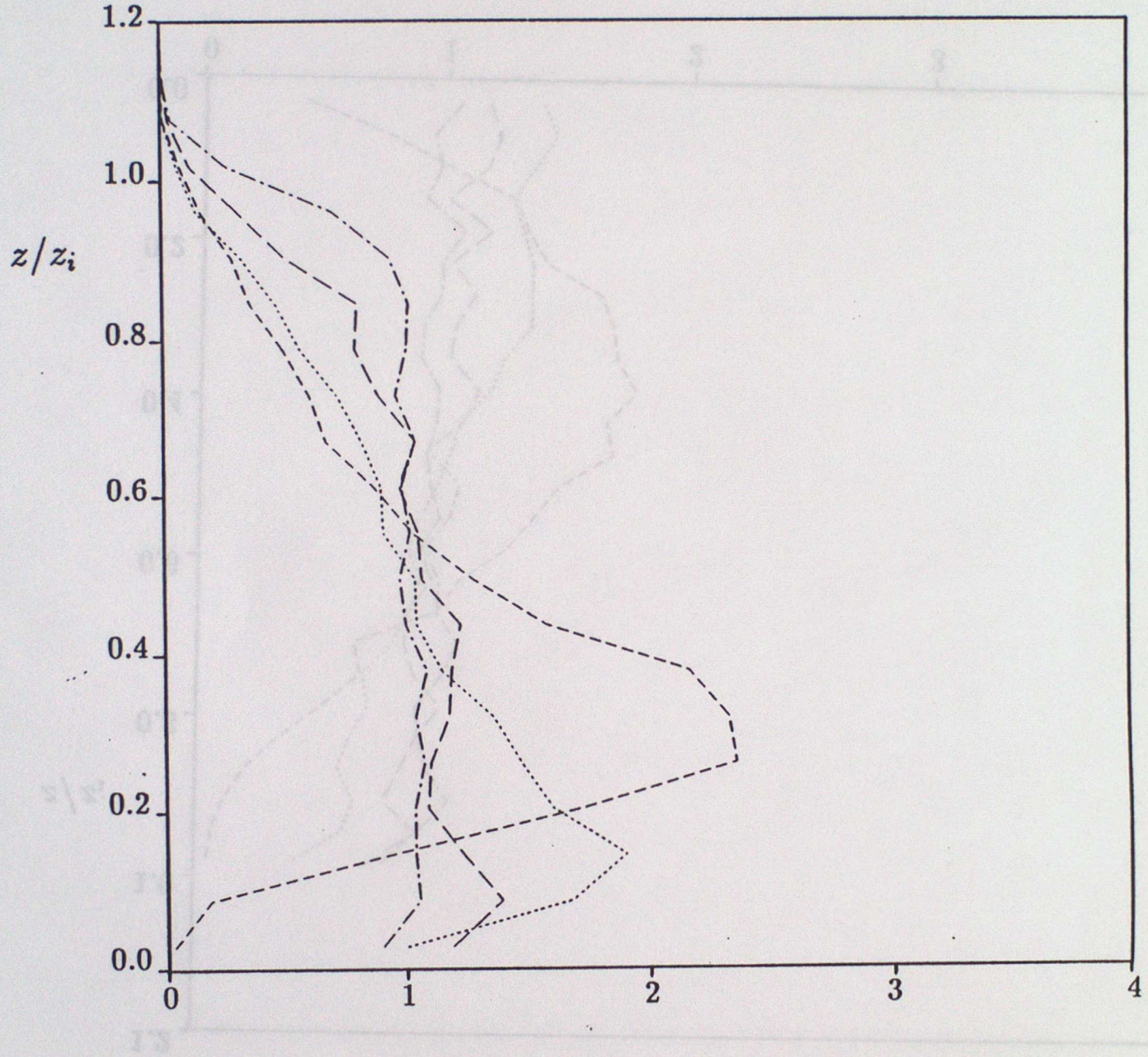

Figure 7d

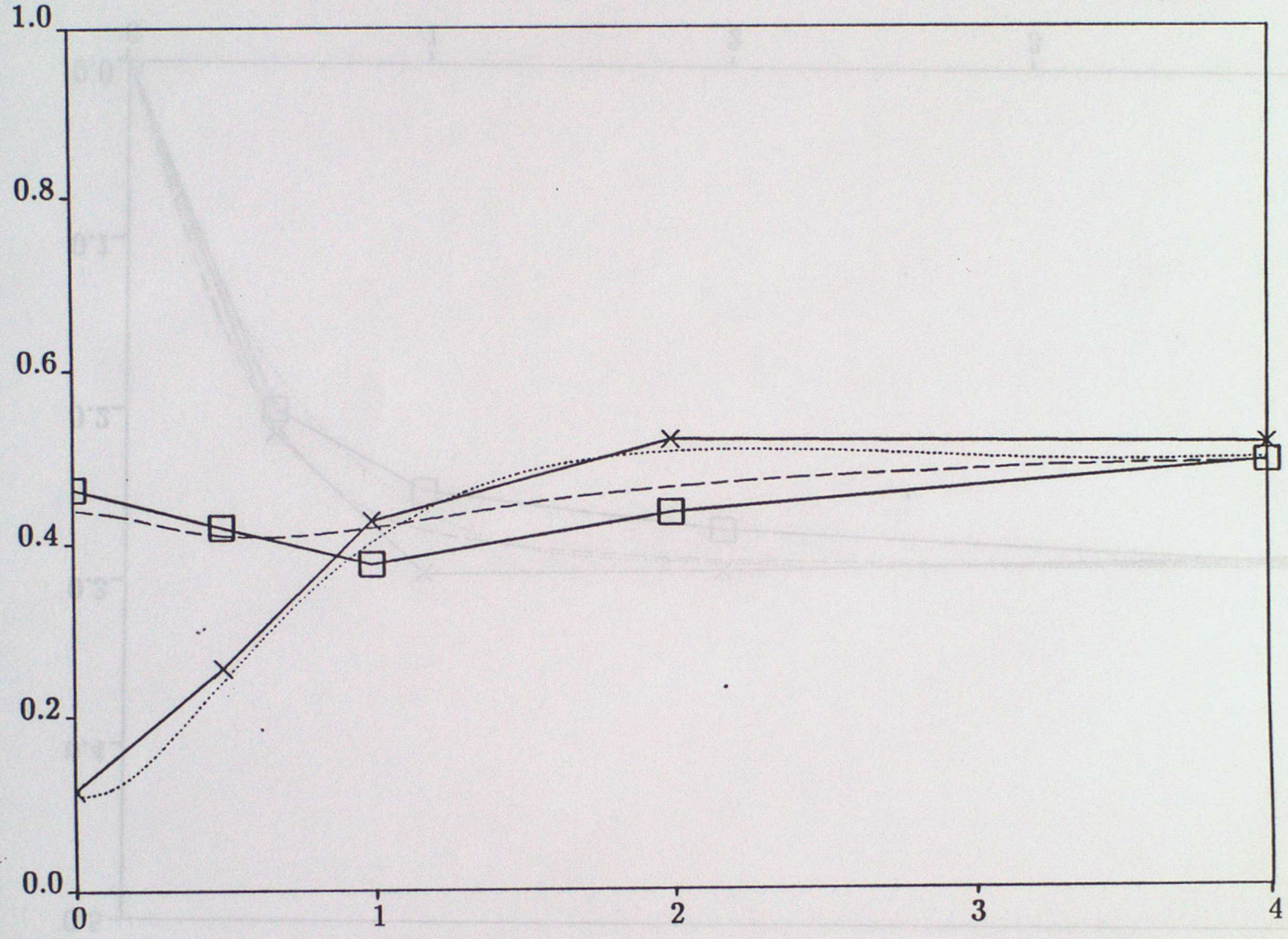

Figure 8a

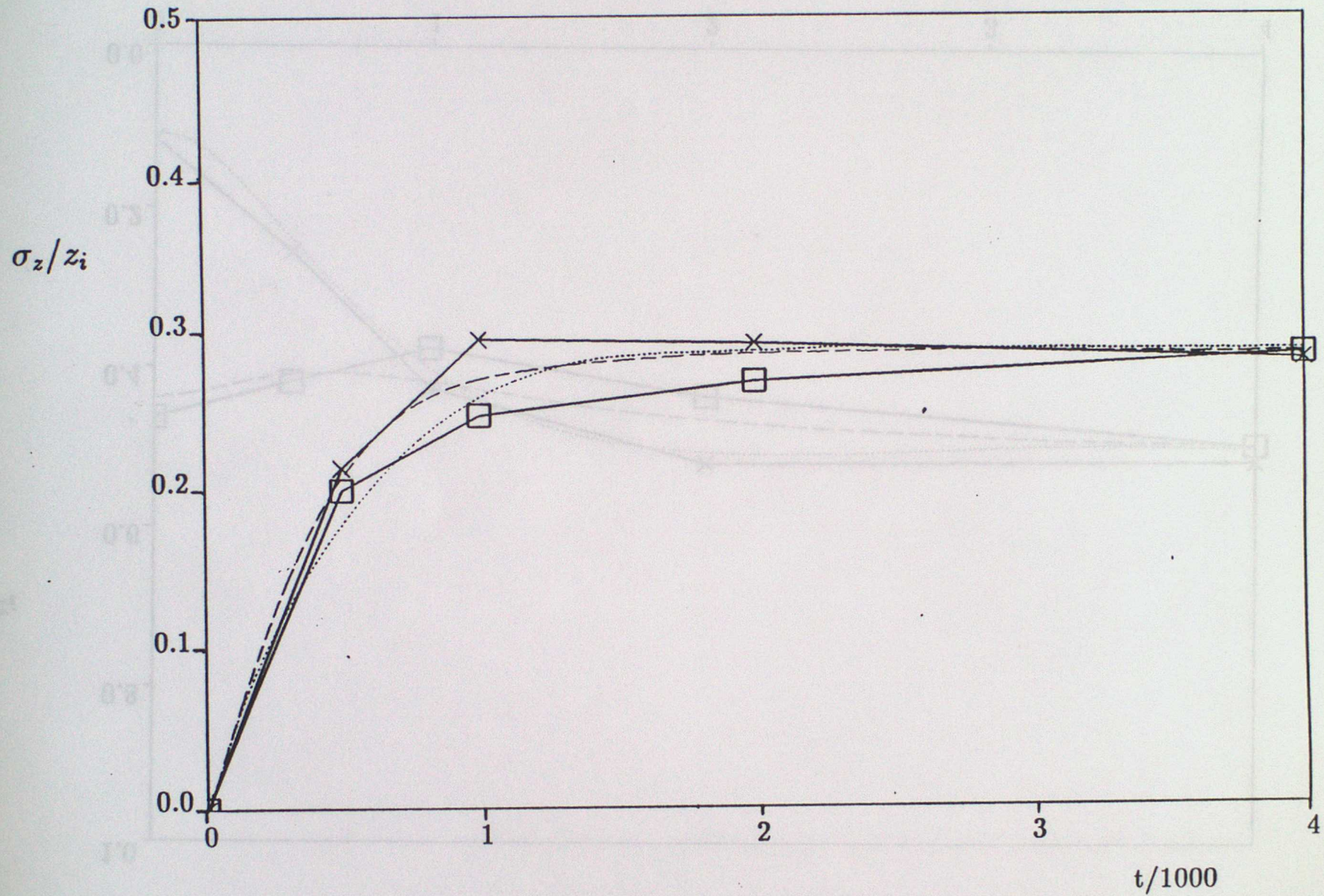

Figure 8b

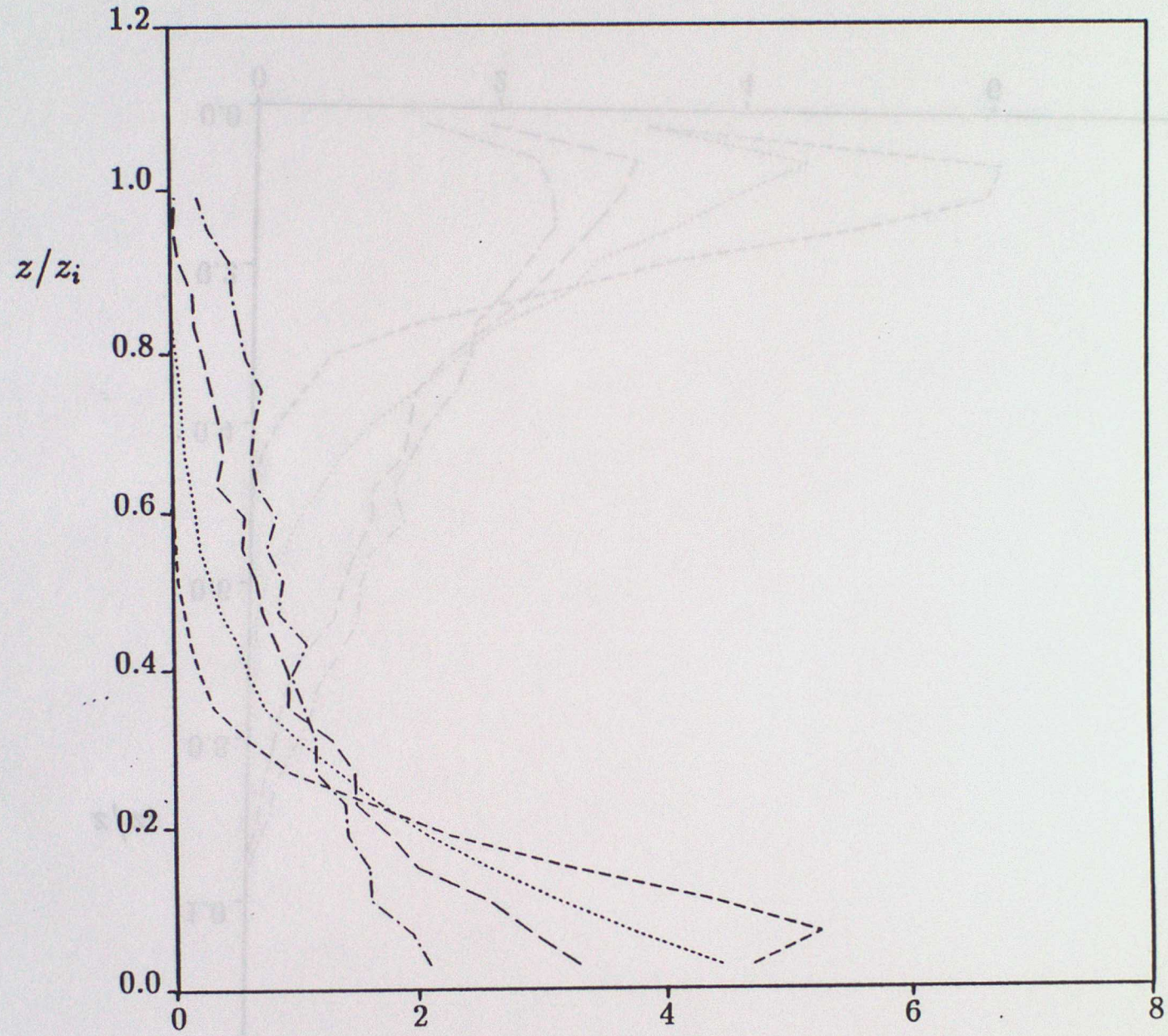

Figure 9a

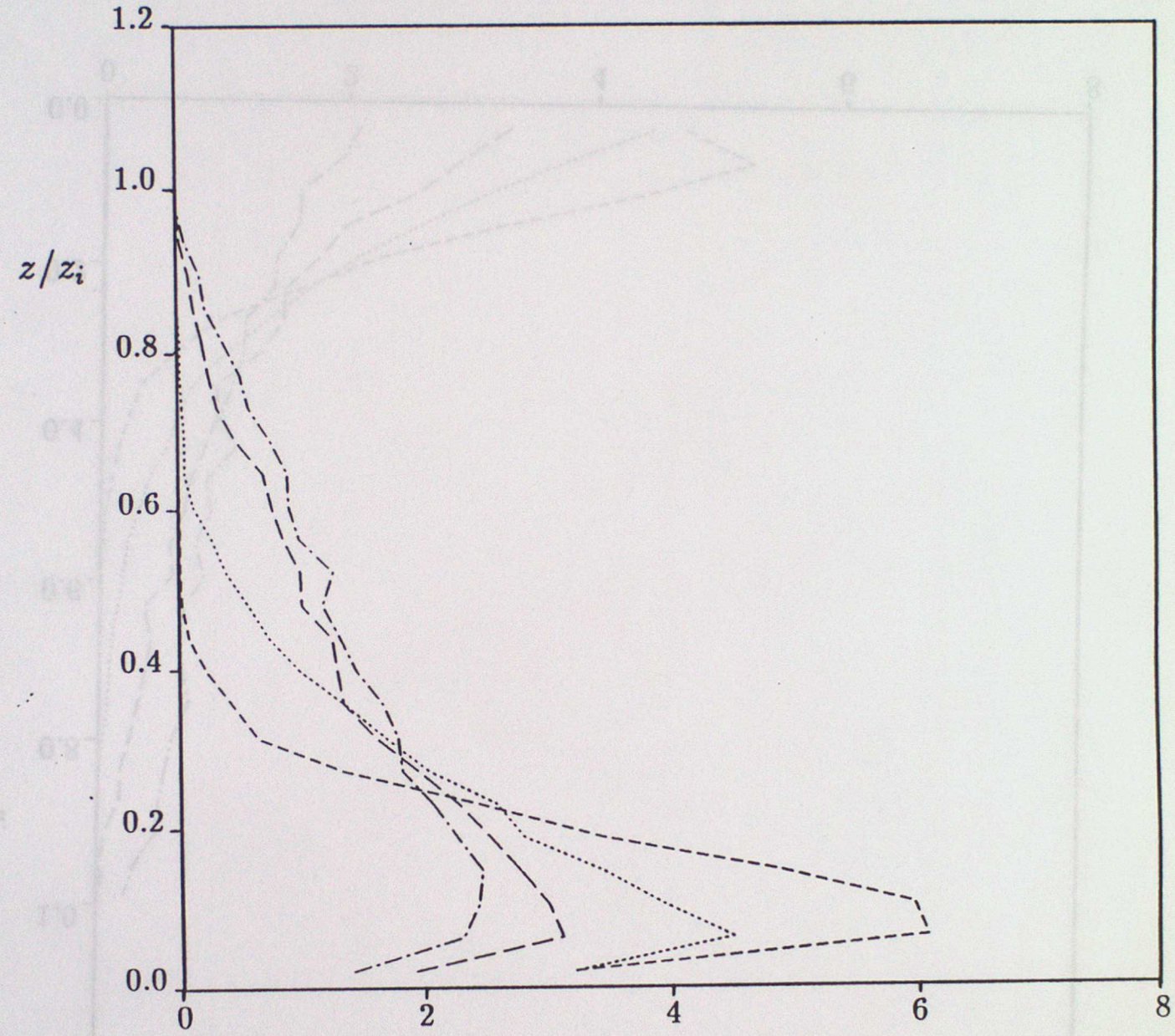

Figure 96

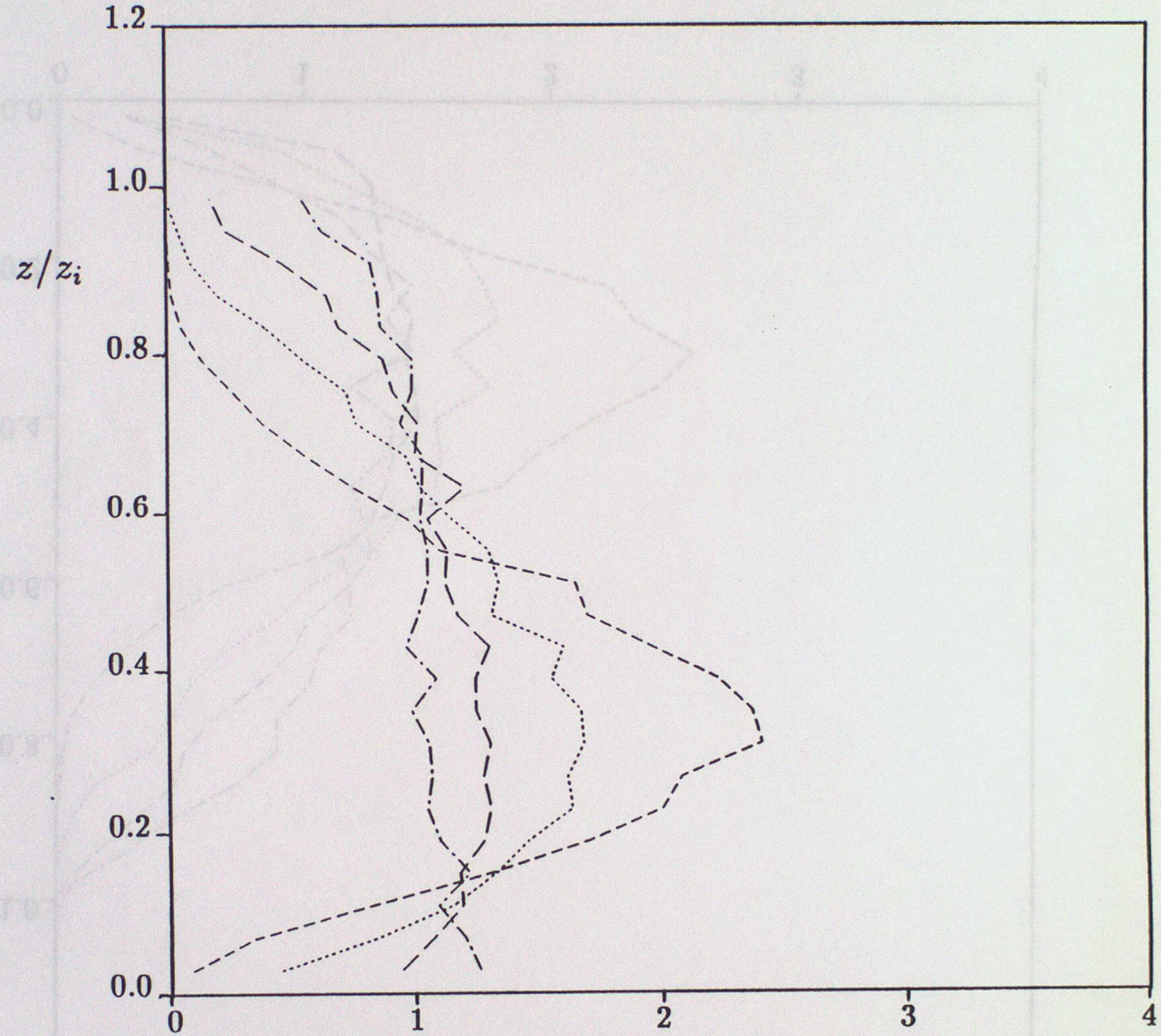

Figure 9c

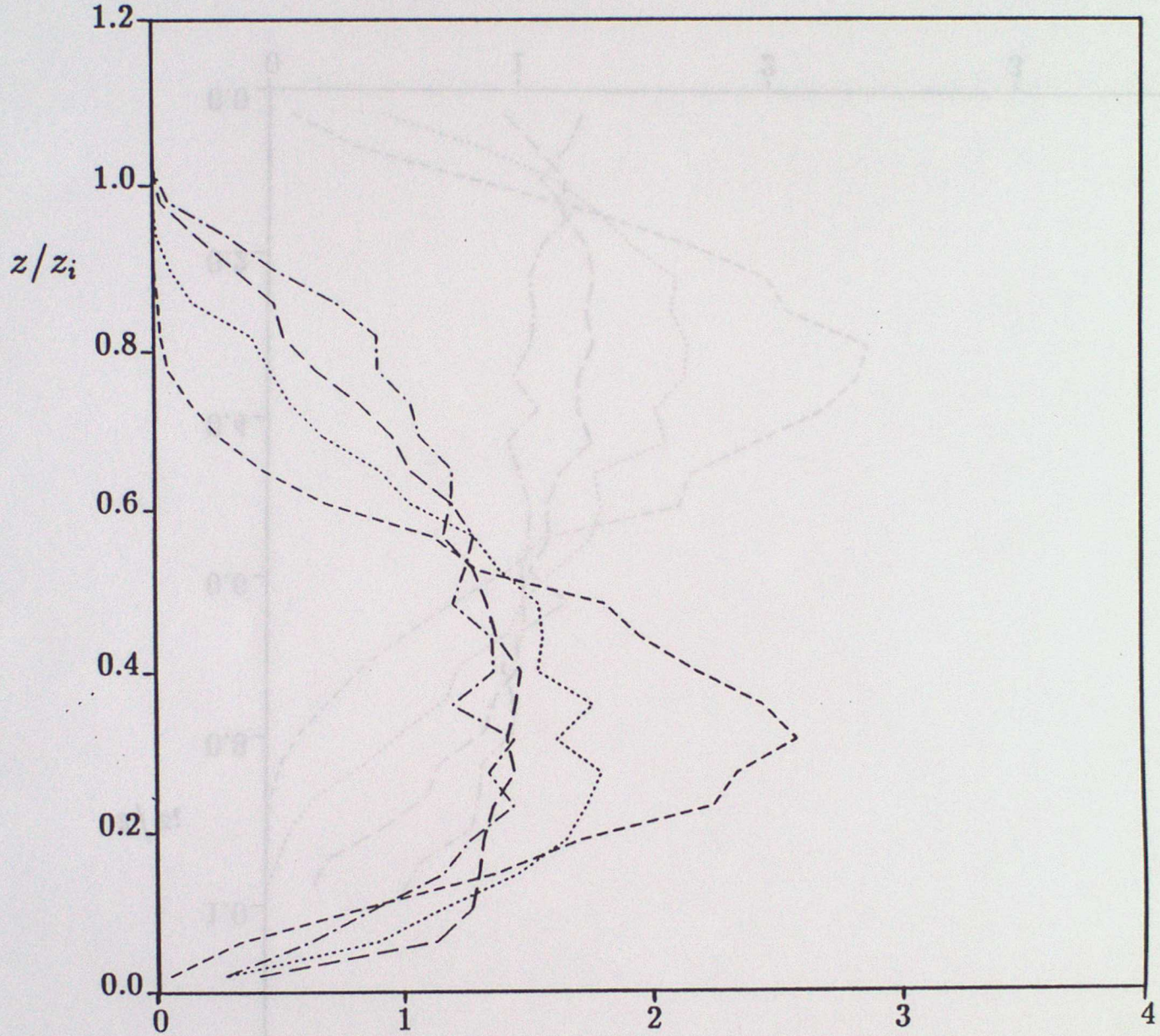

Figure 9d

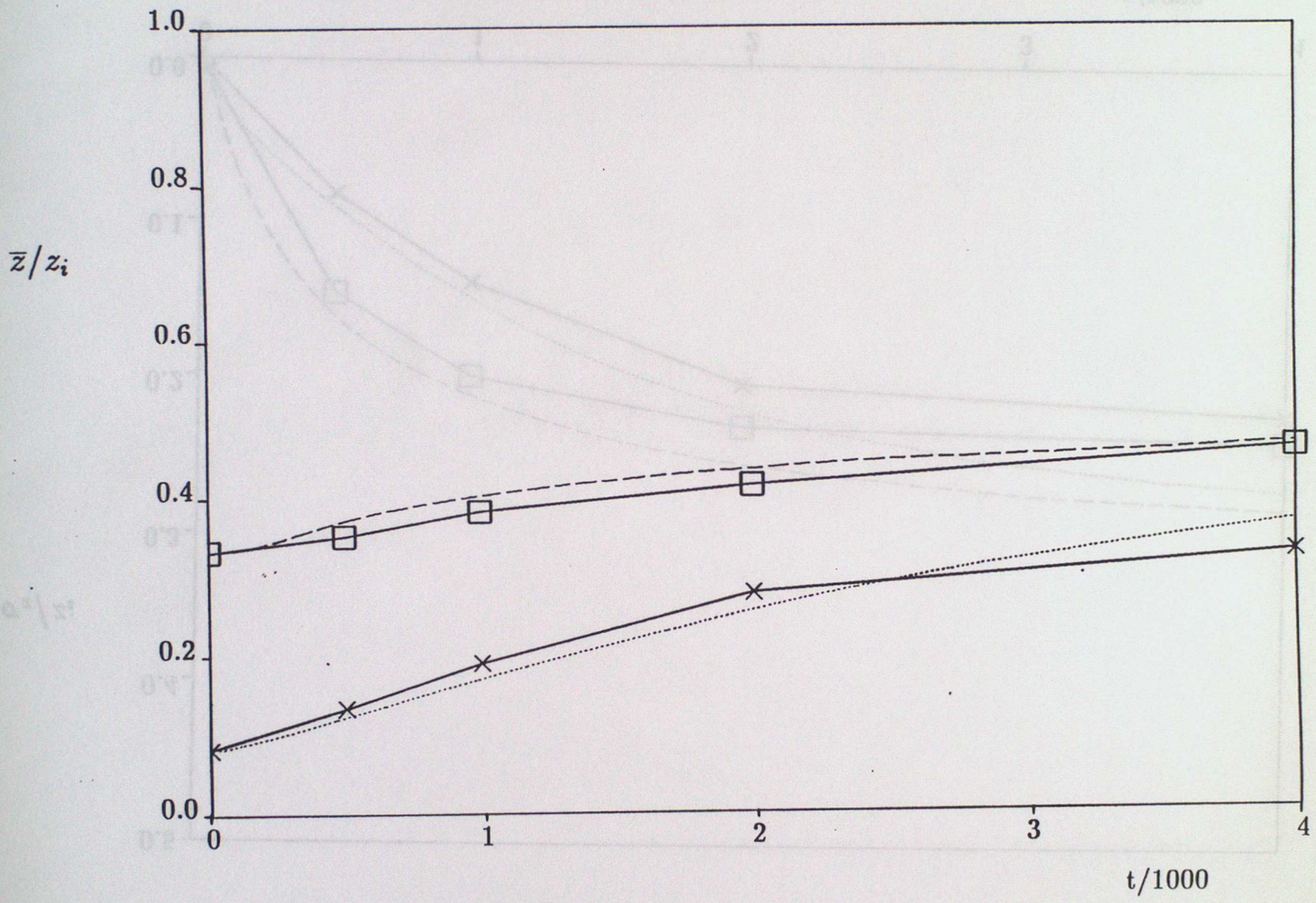

Figure 10a

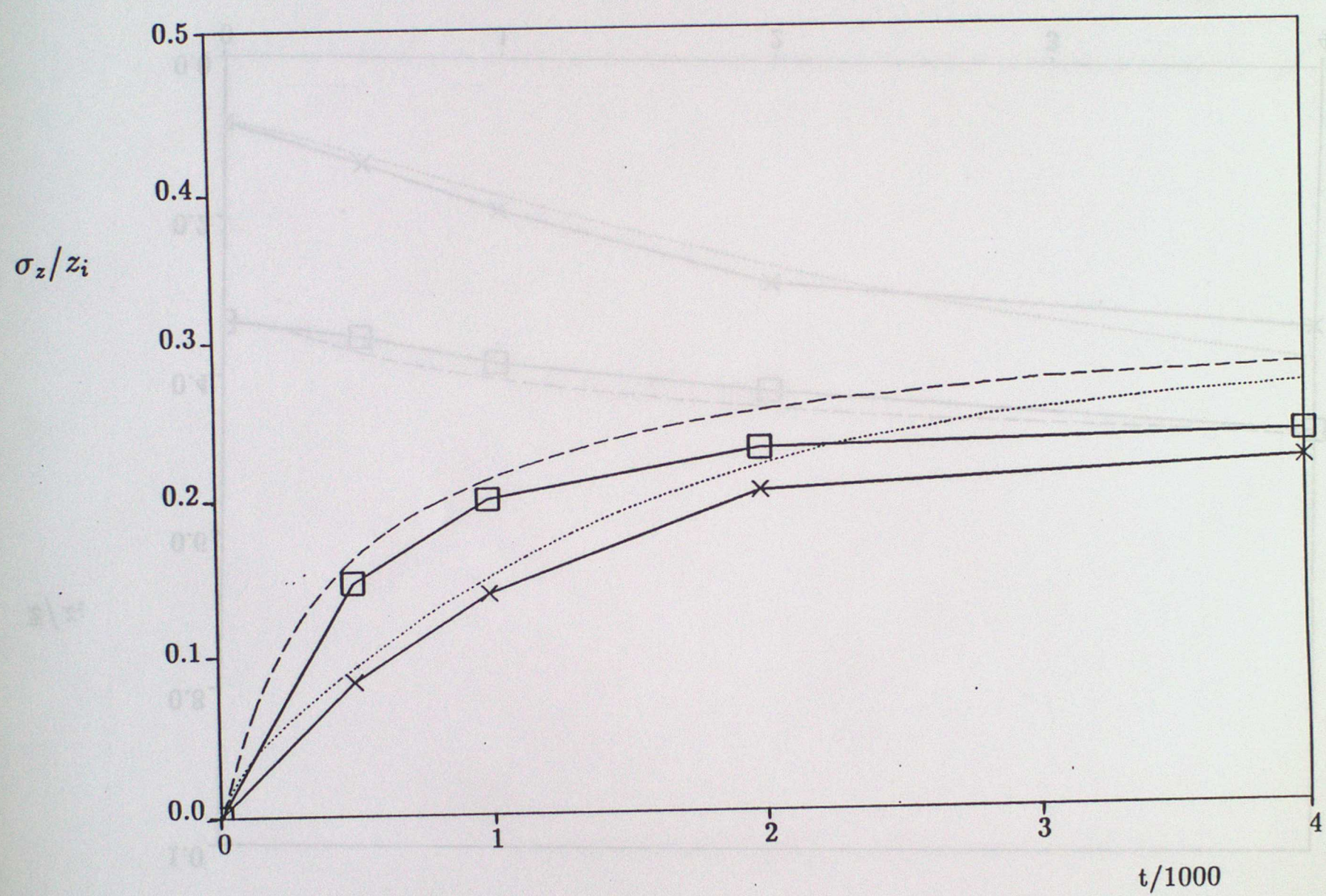

Figure 106

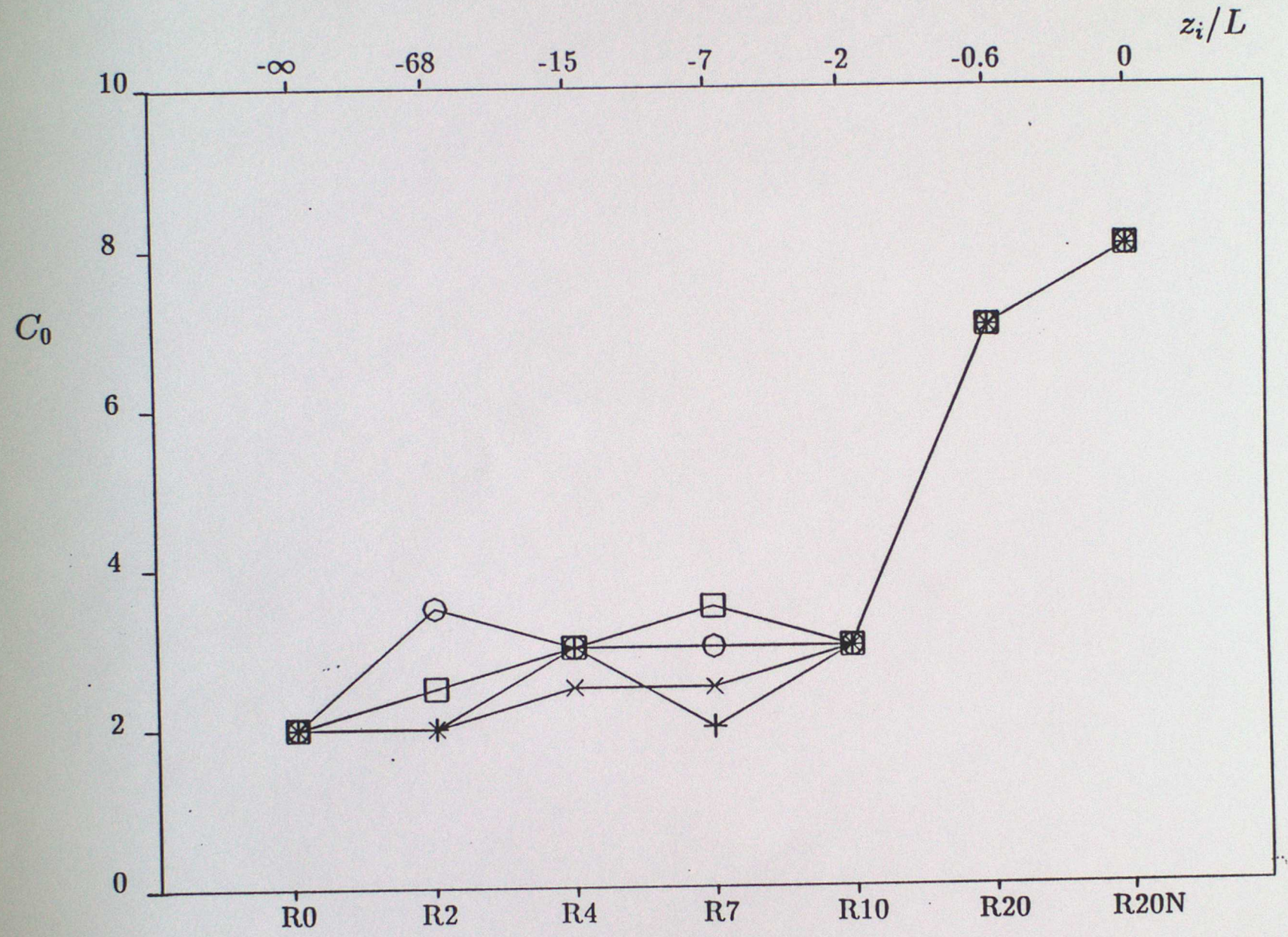

Figure 11